NAVAL POSTGRADUATE SCHOOL
Monterey, California

THESIS

A STUDY ON HYDROGRAPHIC CONDITIONS AND SALT BUDGET CALCULATION FOR THE GULF OF FARALLONES WITH THE DATA COLLECTED IN AUGUST 1990

by

Erhan Gezgin

MARCH 1991

Thesis Advisor: Curtis A. Collins
Co-Advisors: Leslie Rosenfeld
Frank Schwing

SECURITY CLASSIFICATION OF THIS PAGE

REPORT DOCUMENTATION PAGE

Form Approved OMB No 0704-0188

1a. REPORT SECURITY CLASSIFICATION: Unclassified	1b. RESTRICTIVE MARKINGS
2a. SECURITY CLASSIFICATION AUTHORITY	3. DISTRIBUTION/AVAILABILITY OF REPORT: Approved for public release: Distribution is unlimited
2b. DECLASSIFICATION/DOWNGRADING SCHEDULE	
4. PERFORMING ORGANIZATION REPORT NUMBER(S)	5. MONITORING ORGANIZATION REPORT NUMBER(S)
6a. NAME OF PERFORMING ORGANIZATION: Naval Postgraduate School; 6b. OFFICE SYMBOL (If applicable): OC	7a. NAME OF MONITORING ORGANIZATION: Naval Postgraduate School
6c. ADDRESS (City, State and ZIP Code): Monterey, CA 93943-5000	7b. ADDRESS (City, State, and ZIP Code): Monterey, CA 93943-5000
8a. NAME OF FUNDING/SPONSORING ORGANIZATION; 8b. OFFICE SYMBOL (If applicable)	9. PROCUREMENT INSTRUMENT IDENTIFICATION NUMBER
8c. ADDRESS (City, State, and ZIP Code)	10. SOURCE OF FUNDING NUMBER: PROGRAM ELEMENT NO. / PROJECT NO. / TASK NO. / WORK UNIT ACCESSION NO.

11. TITLE (Include Security Classification)
A STUDY ON HYDROGRAPHIC CONDITIONS AND SALT BUDGET CALCULATION FOR THE GULF OF FARALLONES WITH THE DATA COLLECTED IN AUGUST 1990

12. PERSONAL AUTHORS
ERHAN GEZGIN

13a. TYPE OF REPORT	13b. TIME COVERED	14. DATE OF REPORT (Year, Month, Day)	15. PAGE COUNT
Master's Thesis	FROM_____ TO_____	MARCH 1991	93

16. SUPPLEMENTARY NOTATION
The views expressed are those of the author and do not reflect the official policy or position of the Department of Defense or the U.S. Government

17. COSATI CODES			18. SUBJECT TERMS (Continue on reverse if necessary and identify by block numbers)
FIELD	GROUP	SUB-GROUP	hydrographic conditions of Gulf of Farallones

19. ABSTRACT (Continue on reverse if necessary and identify by block numbers)

The circulation pattern observed in the Gulf of Farallones on 5-10 August 1990 was a cyclonic system of flow. Water entered the Gulf from south of the Farallon Islands and left the Gulf between Pt. Reyes and the Farallon Islands. This pattern is confirmed by a satellite image which indicates a tongue of warm water penetrating into the Gulf from offshore as well as the increasing salinity and density along a shallow salinity minimum in this area. This cyclonic flow was also observed by previous current meter moorings in and near the Gulf. Note that this circulation would provide a return flow to balance offshore flow which has been observed at Pt. Reyes.

20. DISTRIBUTION/AVAILABILITY OF ABSTRACT	21. ABSTRACT SECURITY CLASSIFICATION	
XX UNCLASSIFIED/UNLIMITED __ SAME AS RPT __ DTIC USERS	unclassified	
22a. NAME OF RESPONSIBLE INDIVIDUAL: Curtis A. Collins	22b. TELEPHONE (Include Area Code): (408) 646-2673	22c. OFFICE SYMBOL: OC/Co

DD Form 1473, JUN 86 *Previous editions are obsolete.* SECURITY CLASSIFICATION OF THIS PAGE

S/N 0102-LF-014-6603 Unclassified

Approved for public release: Distribution is unlimited

A Study on Hydrographic Conditions and Salt Budget Calculation for the Gulf of Farallones with the Data Collected in August 1990

by

Erhan Gezgin
Lieutenant Junior Grade, Turkish Navy
B.S., Turkish Naval Academy, 1985

Submitted in partial fulfillment
for the degree of

MASTER OF SCIENCE IN
PHYSICAL OCEANOGRAPHY

from the

Naval Postgraduate School

March 1991

Author: _____
Erhan Gezgin

Approved by: _____
Curtis A. Collins, Thesis Advisor

_____
Leslie Rosenfeld, Co-Advisor

_____
Frank Schwing, Co-Advisor

_____
Curtis A. Collins, Chairman
Department of Oceanography Science

ABSTRACT

The circulation pattern observed in the Gulf of Farallones on 5-10 August 1990 was a cyclonic system of flow. Water entered the Gulf from south of the Farallon Islands and left the Gulf between Pt. Reyes and the Farallon Islands. This pattern is confirmed by a satellite image which indicates a tongue of warm water penetrating into the Gulf from offshore as well as the increasing salinity and density along a shallow salinity minimum in this area. This cyclonic flow was also observed by previous current meter moorings in and near the Gulf. Note that this circulation would provide a return flow to balance offshore flow which has been observed at Pt. Reyes.

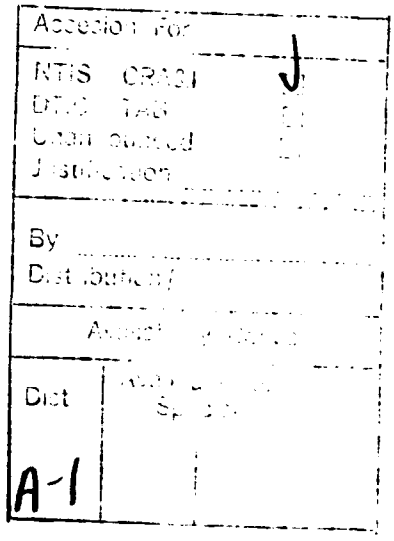

TABLE OF CONTENTS

LIST OF TABLES

LIST OF FIGURES

ACKNOWLEDGMENT

I would like to express my gratitude to my thesis advisor Curtis A. Collins and to my co-advisors Dr. Leslie Rosenfeld and Dr. Frank Schwing for their help and guidance with my thesis. I also thank Prof. T. Garfield, Paul Jessen and Tarry Rago for their help and support.

I. INTRODUCTION

The Gulf of Farallones (Figure 1) is an important fishing, shipping and recreational area off San Francisco Bay, the fourth largest urban area in the United States. It is a region of the continental shelf bounded by the Farallones Islands on the west, and extending from Pt. Reyes in the north to Pigeon Point in the south. From a physical oceanography perspective, the most important process which occurs in this region is the exchange of water between the Gulf and San Francisco Bay. Drifter studies have shown that surface flow from the Bay mixes with oceanic waters, and subsurface water from the Gulf flows into San Francisco Bay (Conomos, 1979). Satellite photographs have shown that plumes of warm sediment-laden water from the Bay occasionally extend most of the way to the Farallones (Minerals Management Service, 1987).

Obviously, these estuarine waters from San Francisco can carry a variety of pollutants into the Gulf of Farallones. Pollutants have also been introduced more directly to the Gulf; because of the proximity of the region to the Bay, the Gulf and the adjacent slope have been used as dump sites. Offshore dump sites were used by the Navy for low level atomic wastes from the Radiological Laboratory Alameda and a survivor of the hydrogen bomb tests at Eniwotok, the **USS Independence**, was scuttled in this area as well. The designation of the

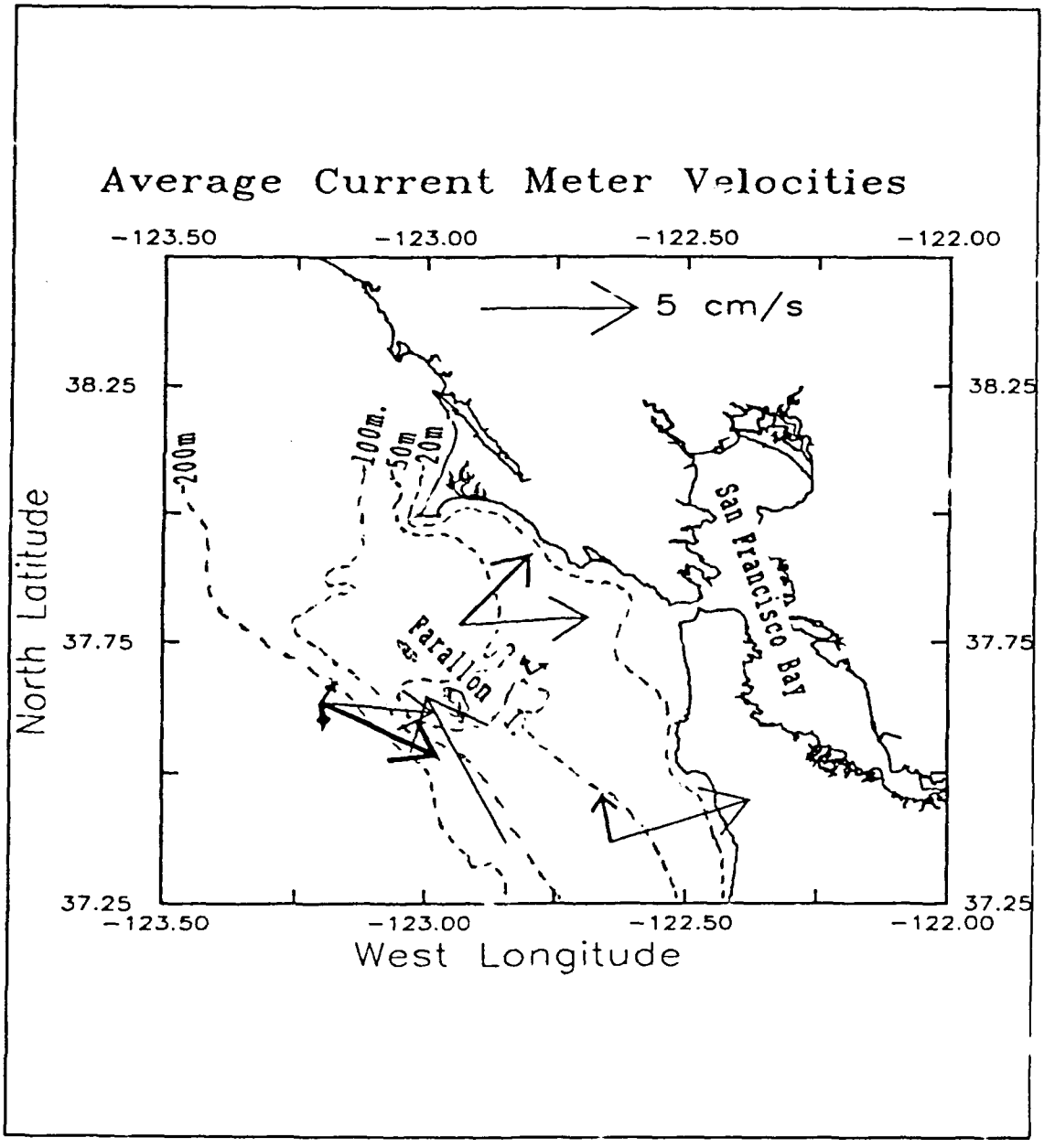

Figure 1. Mean Currents in the Region of the Gulf of the Farallones. Data are vector averages from current meters which were moored for 6 weeks or longer. Vectors thicken with depth at a given station. Vectors plotted include results from a Navy slope mooring at 37.6°N, 123.2°W for 285m, 485m, 885m, and 1685m (Noble, 1990), super CODE moorings at 37.4°N, 122.6°W for 35m and 65 m and at 37.4°N, 122.8°W, for 105m (Denbo, et al., 1984), and from sediment transport studies for 30m and 40m at 37.7°N, 122.8°W and for 30m and 59m at 37.8°N, 122.9°W (Noble and Gelfenbaum, 1990).

Farallones as a National Marine Sanctuary, as well as a growing awareness of the marine environment, have resulted in more carefully regulated ocean dumping. Our studies were stimulated by a Navy need to know more about the region prior to dumping sediment spoils from ship channels at NAS Alameda and NSC Oakland.

A. OCEAN CIRCULATION IN THE GULF OF FARALLONES

Despite the obvious importance of the region, there have been few modern measurements in the Gulf. During the Super CODE experiment, current measurements were made on the continental shelf at five locations along the West Coast of the United States (Strub, et al., 1987). One of these moorings was located off San Francisco from April 1981 to August 1982 at 37.4N, 122.3W in 80m of water. Currents were measured at depths of 35m and 65m. The lower current meter indicated poleward mean alongshore flow; although there was more variability at the upper instrument, onshore mean currents were observed (Figure 1). The magnitude of the fluctuations and seasonal variability was much less at this site than the current meter moorings at other Super Code locations.

Measurements were also made during the Central California Circulation Study (Chelton, et al., 1987); these included CTD and current meter measurements. The CTD stations extended in a line offshore from station 270 at 37-21.9N, 122-30.2W to station 278 at 37-03N, 123-11.2W, a distance of about 85km.

This transection included the two onshore CTD stations of CALCOFI line 63. CTD data were collected in February, July and October 1984, and in January 1985. Two moorings in this area were also located along this transection, one at the 100m isobath on the shelf and the other at the 500m isobath on the slope; current meter observations were made at a depth of 70m from February 1984 through July 1985. On the shelf, the flow was generally equatorward. However in both studies the magnitude of the synoptic-scale fluctuations were much greater than the seasonal signal.

More recently, the USGS has begun a series of investigations to better understand the distribution of sediments in the Gulf. In this study, two current meter moorings were deployed in the central portion of the Gulf of Farallones from May 4 1989 through October 13 1989 at 37-41.18N, 122-47.78W and 37-47.03N, 122-56W. Both moorings had two vector averaging current meters, one at 30m and the other ones at 49m and at 59m, respectively, which were about 5m above the bottom (30m data are used below to remove tidal effects from the ADCP data used in this thesis). These measurements yielded consistent shoreward flow at the northern site; this onshore flow was weaker but still persistent at the southern site (Figure 1). Alongshelf currents at both locations were directly toward the northwest from August through October. Tidal currents dominated the current record

with diurnal and semi-diurnal tides containing 29 to 58% of the energy (Noble and Gelfenbaum, 1990).

The direct measurements of long-term circulation (Figure 1) in the Gulf indicate onshore flow. How do the waters from San Francisco mix and exit the Gulf? For this reason, data were collected to undertake transport and salt-flux calculations, and to estimate the residence time of Gulf waters.

B. CALIFORNIA CURRENT SYSTEM

Processes in the Gulf must also be understood in the context of regional circulation patterns associated with the California Current System. These patterns dominate the circulation over the continental slope to the west of the Farallones. The California Current System is a part of the great clockwise circulation of the North Pacific Ocean. The California Current transports water of relatively low temperature and salinity and high dissolved oxygen and nutrients from the subarctic toward the tropics (Hickey, 1979).

The two other primary currents off central California are the California Undercurrent and the Davidson Current. The poleward flowing Undercurrent transports water of relatively high temperature, salinity and nutrients and low dissolved oxygen from equatorial regions (Hickey, 1979). The Undercurrent is trapped along the continental slope within 45-

60 miles of the coast off Point Sur (Chelton, 1984). Northward flow extends to the surface from October through February. This portion of the poleward flow is referred to as the Davidson Current. A second weaker period of northward surface current is noted in late summer over the slope off San Francisco and Monterey. The Undercurrent is weakest in spring and early summer. Velocities of up to 14cm/s occur near the surface in December.

While this description gives a general view of the large scale current patterns off central California, mesoscale and smaller scale variability will also affect this region.

C. ORGANIZATION

This thesis will describe physical oceanographic data which were collected during August 1990 in the Gulf of the Farallones by personnel from the Naval Postgraduate School and National Marine Fisheries Service. The purpose of the measurements was to describe the circulation patterns in the region of the Farallones.

After this chapter, the thesis is organized as follows. Chapter II describes instrumentation and data collection. Chapter III explains calibration and the processing of the data. Chapter IV describes the resulting hydrographic conditions. Chapter V describes the salt and mass budgets for the Gulf of Farallones. Chapter VI summarizes the results and conclusions of this study.

II. DATA COLLECTION AND INSTRUMENTATION

A. CRUISE PLAN

On August 5-10, 1990, the **R/V Pt. Sur** collected physical oceanographic data in the Gulf of Farallones and over the adjacent continental slope. As shown in Figure 2, data collection was organized along four transections. Two of these sections are more or less parallel to isobaths and are referred to as "inshore" and "offshore", the latter being farthest from the coast and in the deepest water. The other two sections are perpendicular to the bathymetry; the northern transection passes north of North Farallon Island and is referred to as the "Farallones" transection. The southern transection passes over Pioneer seamount and intersects the coast at Pt. San Pedro, and is called the "Pioneer" transection. Station spacing along these transections varied from 1.7km to 12.4km; stations were planned so that stations were closest together where topography was steepest over the continental slope.

The **R/V Pt. Sur** departed Moss Landing at 0935 PDT on 5 August, steaming directly to the first station which was on the 100 fathom isobath southwest of Pigeon Point (Figure 2). Stations were occupied sequentially except between stations 18 and 22 when stations 21, 20, and 19 were occupied, in that

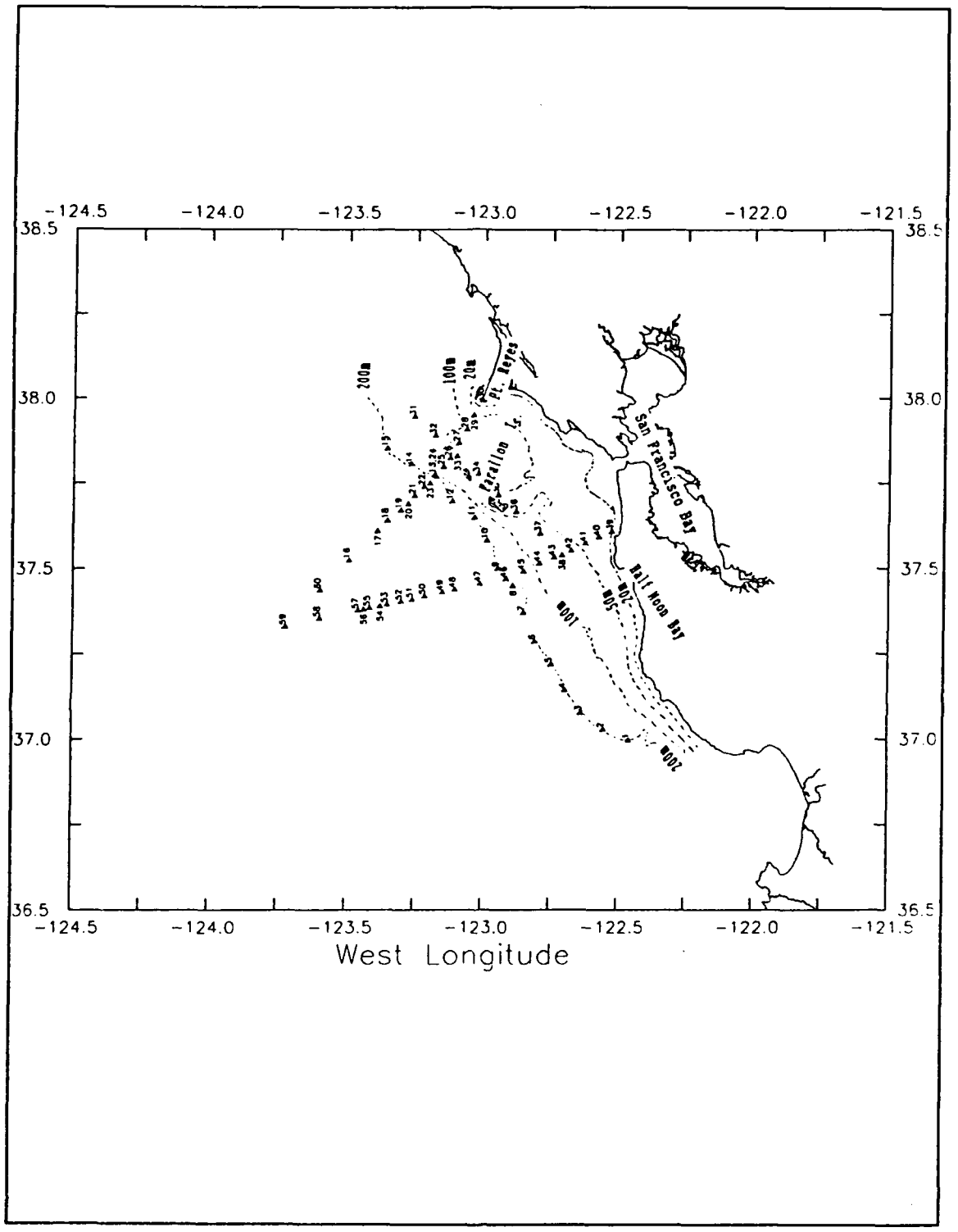

Figure 2. Location of Hydrographic Stations: Stations occupied during the 5-10 August 1990 Survey. Isobaths (in meters) are indicated by dotted lines.

order. After completion of station 60, Pegasus velocity data were collected near station 18, and the **R/V Pt. Sur** then returned to Moss Landing, arriving at 1056 PDT on 10 August. Details on the geography of the sections, the station locations, and the observational methods are given below.

B. BATHYMETRIC CONDITIONS ALONG THE TRANSECTIONS

The inshore transection, which is about 65km long, has 8 stations approximately 9 km distant from each other. The entire transection is over the shallow waters of Gulf of Farallones, and the depths of stations vary between 47m and 85m.

The offshore transection is 130km long and has 15 stations at approximately 9km spacing. Although this transection was planned to follow the 100 fathom (183m) isobath, because of the complexity of the bottom topography and strong breezes and drift while on station, three stations are deeper than 250m on this transection.

The Farallon Islands transection consists of 17 stations. The transection begins at Pt. Reyes, runs just south of Fanny Shoal, and thence offshore, perpendicular to the continental slope. Since it is a cross-shelf transection, the distance between stations varies. The six inshore stations (30-25) are on the continental shelf in water depth of less than 81m. The distance between shelf stations along this transection varies from 3.9km to 5.7km. Station 25 is located just south of Fanny

Shoal in 55m of water. Station 26 is located offshore of Fanny Shoal in 119m of water. The rest of the transection lies over the continental slope. The total length of this transection is about 100km. Water depth varies from 45m (station 30 at Pt. Reyes) to 3501m at the most offshore station, 59. The distance between stations over the slope varies between 1.9km to 16.2km.

The 113 km long Pioneer Seamount transection is also a cross-shelf transection. It shares station 59 with the Farallones transection and has a total of 22 stations which are spaced in order to have measurements at particular isobaths. In this transection the first seven inshore stations (39-45) are over the continental shelf in water shallower than 100m. The distance between the shelf stations varies from 2.6km to 5.6km. Stations 46 through 52 are over the continental slope, stations 53 to 56 are over Pioneer seamount, and the final three stations (57 to 59) are on the outer continental slope where water depth decreases from 2237m to 3501m. The distance between the slope stations varies from 1.7km to 12.4km. The shallowest station over Pioneer Seamount was station 55 where the water depth was 950m.

C. INSTRUMENTS USED FOR DATA COLLECTION

1. Conductivity-Temperature-Depth (CTD) Soundings

Soundings of conductivity and temperature were obtained at 60 stations using a Neil Brown MK III CTD. This

instrument is considered to have an accuracy of ±.005 C (temperature), ±.005 PSU (salinity) and ± 3.2 dbar (pressure), with a resolution of .0005 C, .001 PSU and 0.05db. At each station the CTD was lowered continously to within 5-30m of the bottom and then halted at certain depths during retrieval to collect sea water samples for calibration. Station locations for each of the transections, time and date, and water depth are provided in Tables I-IV.

2. Acoustic Doppler Current Profiler (ADCP)

The **R/V Pt. Sur** was outfitted with a RD Instrument 150 kHz ADCP. with a four beam Janus array. ADCP data were collected continuously along all four transects.

The ADCP measures sea water velocities relative to the ship by measuring the Doppler shift between the outgoing acoustic signal and returning signal for each of four beams. The velocities of targets in the sea water such as plankton and air bubbles are assumed to be random so that averaging of these velocities gives a Gaussian spectrum centered at the Doppler frequency which corresponds to the relative velocity of the water. This relative velocity is recorded as "u" and "v" components of velocity relative to the platform and averaged over 3 to 5 minutes. The velocity components are defined as "u" being positive eastward and "v" being positive northward. These relative velocities are converted to true velocities by using navigation data to determine the velocity

of the ship. The most important factor in ADCP data processing is to have accurate navigation data for the calculation of the true velocities. Small errors in navigation data can cause severe errors in the magnitude of absolute velocities. Comparisons of navigation methods in this region (Moschovos, 1989) indicate that 20 minute averaging times yield errors of about 1 cm/s.

The ADCP measures the velocity components of the sea water under the ship with a range from 6m beneath the ship's keel to about 400m depth depending on the strength of the return signals. The system was set to have a vertical resolution of 4m.

The methods of Pollard and Read (1989) were used for angular calibration; accuracy of the vessel heading is estimated to be 0.2° which gives an accuracy of 1-2 cm/s in the cross-track velocity component for a ship speed of 9 knots. As discussed below, conservation of volume for the Gulf of Farallones yields an accuracy of 3 cm/s for ADCP data collected on this cruise.

TABLE I. CTD STATIONS ALONG THE OFFSHORE TRANSECTION

STATION #	LOCATION	DATE/TIME	DEPTH
1	36°58.60'N 122°28.08'W	8/5 13:45	191M
2	37°00.52'N 122°33.74'W	8/5 14:46	188M
3	37°03.46'N 122°38.69'W	8/5 15:53	255M
4	37°07.47'N 122°42.32'W	8/5 16:58	284M
5	37°11.96'N 122°45.37'W	8/5 17:56	212M
6	37°15.98'N 122°49.00'W	8/5 18:54	179M
7	37°21.06'N 122°51.56'W	8/5 19:58	177M
8	37°25.72'N 122°53.93'W	8/5 20:59	177M
9	37°28.86'N 122°57.38'W	8/5 21:53	183M
10	37°33.72'N 122°59.77'W	8/5 23:08	186M
11	37°37.74'N 123°02.70'W	8/6 00:02	162M
12	37°40.65'N 123°07.57'W	8/6 01:22	195M
13	37°45.00'N 123°11.20'W	8/6 02:37	291M
14	37°47.19'N 123°16.77'W	8/6 04:01	200M
15	37°49.95'N 123.22.05'W	8/6 05:04	163M

TABLE II. CTD STATIONS ALONG THE INSHORE TRANSECTION

STATION #	LOCATION	DATE/TIME	DEPTH
31	37°55.57'N 123°16.03'W	8/8 04:24	85M
32	37°52.24'N 123°11.37'W	8/8 05:30	78M
33	37°48.70'N 123°06.52'W	8/8 06:34	56M
34	37°45.38'N 123°01.87'W	8/8 07:35	56M
35	37°41.75'N 122°57.45'W	8/8 08:40	47M
36	37°38.84'N 122°53.37'W	8/8 09:40	68M
37	37°35.00'N 122°48.00'W	8/8 10:52	66M
38	37°31.39'N 122°43.06'W	8/8 12:06	66M

TABLE III. CTD STATIONS ALONG THE FARALLONES TRANSECTION

STATION #	LOCATION	DATE/TIME	DEPTH
16	37°30.32'N 123°30.16'W	8/6 08:18	2300M
17	37°35.37'N 123°24.12'W	8/6 10:34	2158M
18	37°37.26'N 123°21.96'W	8/6 12:36	2251M
19	37°39.10'N 123°19.02'W	8/7 02:15	1999M
20	37°40.04'N 123°17.62'W	8/6 23:48	1938M
21	37°41.63'N 123°15.95'W	8/6 22:29	1512M
22	37°43.20'N 123°13.88'W	8/7 05:49	1222M
23	37°43.82'N 123°12.82'W	8/7 10:16	863M
24	37°45.33'N 123°11.53'W	8/7 11:03	119M
25	37°46.71'N 123°09.55'W	8/7 11:40	55M
26	37°48.26'N 123°08.03'W	8/7 12:28	71M
27	37°50.94'N 123°06.17'W	8/7 13:12	81M
28	37°53.32'N 123°04.41'W	8/7 13:49	81M
29	37°55.68'N 123°02.91'W	8/7 14:28	66M
30	37°58.44'N 123°01.14'W	8/7 15:12	45M
60	37°25.03'N 123°36.55'W	8/9 16:46	3279M

TABLE IV. CTD STATIONS ALONG THE PIONEER TRANSECTION

STATION #	LOCATION	DATE/TIME	DEPTH
39	37°35.33'N 122°32.24'W	8/8 13:46	25M
40	37°34.34'N 122°35.05'W	8/8 14:21	35M
41	37°33.24'N 122°37.97'W	8/8 15:07	48M
42	37°32.00'N 122°41.17'W	8/8 15:45	55M
43	37°30.81'N 122°44.87'W	8/8 16:31	71M
44	37°29.76'N 122°48.13'W	8/8 17:09	80M
45	37°28.35'N 122°51.62'W	8/8 17:53	96M
46	37°27.03'N 122°55.49'W	8/8 18:39	178M
47	37°26.11'N 123°01.32'W	8/8 19:45	519M
48	37°25.18'N 123°06.86'W	8/8 20:58	751M
49	37°24.67'N 123°09.55'W	8/8 21:53	907M
50	37°24.00'N 123°13.47'W	8/8 23:07	1232M
51	37°23.38'N 123°16.34'W	8/9 00:14	1490M
52	37°23.01'N 123°18.75'W	8/9 01:30	1897M
53	37°22.45'N 123°21.90'W	8/9 03:07	1657M
54	37°22.28'N 123°23.22'W	8/9 04:28	1057M
55	37°21.90'N 123°25.70'W	8/9 05:32	947M
56	37°21.66'N 123°26.91'W	8/9 06:21	1520M
57	37°21.44'N 123°28.18'W	8/9 07:21	2237M
58	37°20.06'N 123°36.64'W	8/9 09:50	3357M
59	37°18.61'N 123°43.99'W	8/9 12:31	3501M

III. CALIBRATION AND DATA PROCESSING

This chapter describes the steps taken to calibrate and process CTD and ADCP data.

A. CTD

The Neil Brown Mark III CTD was compared with temperature and pressure standards in the Oceanography Department's calibration laboratory on September 15, 1990. This yielded corrections for CTD output as follows:

$$T = .99983*(CTD\ T) + 0.0197$$

$$P = .99946*(CTD\ P)$$

Our standards are believed to be accurate to 0.005 C and 3.2 db.

The CTD was also tuned to measured conductivity within about 0.01 mmho in the calibration lab. Final salinity calibration was done by using in situ salinity samples. Salinity samples are collected at two or three depths on each CTD upcast. Bottle and CTD salinities are compared, obviously bad bottle data discarded, and CTD salinities corrected using a linear regression; corrected CTD salinities are again compared with bottle salinities, data greater than two standard deviations from a linear regression discarded, and then corrected again; this process was then repeated a third time. The standard deviation between bottle and final

corrected CTD salinities was 0.007 psu, which is about twice the 0.003 psu accuracy specified by the CTD manufacturer.

After calibration, waterfall plots of temperature and salinity are produced. Data are examined for bad points or spikes; these are removed and replaced by linearly interpolated values.

Finally, CTD data are averaged into 2m bins.

B. ACOUSTIC DOPPLER CURRENT PROFILER

ADCP data are processed using methods discussed by Kosro (1985). The first step in the ADCP processing was the correction of the navigation data and the calculation of the ship's velocity. Ship's velocity was calculated as "u" and "v" components.

The next step was to determine a reference layer. In this study, the reference layer was chosen as three bins wide. Subtracting the ship's velocity from the average velocity within the chosen reference layer yields an absolute reference velocity for each ensemble. The series of absolute reference velocity was then filtered with a low pass Hamming window filter. The cutoff frequency of this filter was 0.04 cycles per minute (period 25 minutes). Once the absolute reference velocity is determined, the velocity profiles of each ensemble were adjusted to the reference velocity, yielding the final profiles of absolute water velocity.

1. Detiding

Noble's measurements have shown that tidal currents are strong in the region of the Farallones (Noble and Gelfenbaum, 1990). To better estimate the volume and salt fluxes for the region, it is necessary to correct the measured ADCP currents for tides. This in turn requires a prediction of the tidal currents.

To do this, I used current meter data from three different moorings (mean currents and locations of these moorings are illustrated in Figure 1). The "Navy slope" mooring was located at 37-38N, 123-12W from July 7 to August 21, 1990. This mooring was located at the 2525m isobath and had current meters at 285, 485, 885, and 1685m (Noble, 1990). The other two moorings were located on the continental shelf from May 4 - October 13, 1989. One of these shelf moorings was located at the 55m isobath at 37-41.18N, 122-47.78W and had current meters at 30 and 49m. The other shelf mooring was located at the 65m isobath at 37-47.03N, 122-56W and had current meters at 30 and 59m.

I used the 30m current meters from the two shelf moorings for the tidal current prediction over the shelf. The near-bottom current meters were not used to avoid the effects of bottom friction. From the "Navy slope" mooring, I used the upper two current meters which were at 285m and 485m depths for the prediction of tidal currents over the slope. Since the shipboard ADCP used in this study penetrates the water only to

about 450m depth, the two deeper current meters at 885m and 1685m weren't used.

The current meter data from the selected current meters were processed using a tidal current analysis and prediction software package (Foreman, 1978) and current ellipses were calculated for 36 tidal constituents. The largest five constituents were two diurnal constituents, luni-solar (K1) and principle lunar diurnal (01), and three semi-diurnal constituents, principle lunar (M2), principle solar (S2), and larger lunar elliptic (N2). The amplitudes and phases for these constituents are listed in Table V. On the shelf, the largest amplitude currents were diurnal; the semi-major axis for the K1 was 7.2 cm/s. On the slope, the largest amplitude currents were semidiurnal; the semi-major axis for the M2 constituent was 3.4 cm/s.

Since currents were needed not just for a specific location, but for the Gulf of Farallones generally, the difference in tidal currents meant that it was necessary to consider two regimes, slope and shelf. For the shelf region, the two 30m current meters were used. For the slope region, currents at 285 and 485m were used. After averaging the tidal constants within these regimes, a hourly predicted tidal current was derived (Tide 10, Foreman, 1978) for 5-10 August. These hourly values were interpolated to three-minute values. These three-minute values were subtracted from the measured

ADCP currents. This data series is subsequently referred to as "detided" ADCP data.

2. Flux calculations

Flux calculations required detided ADCP velocities at locations corresponding to CTD stations. For this purpose, a transport program was used. In this program, time intervals were selected so the CTD station was in the middle of the time interval. This allowed the ADCP data to be time averaged. The output of the program is temporally averaged data for each 4m vertical bin. The output of this program was combined with the distance between stations to calculate transports and salt fluxes. A cross-transection velocity was calculated by using midpoints between CTD stations to orient the subsection.

The first observed ADCP value was for the 7-11m depth bin; for transport calculations, this velocity was assumed for the entire surface to 11m depth bin. At the bottom, the last ADCP observation was assumed to be the bottom value. This latter approximation means that the bottom 15% of the water column was not included in transport estimates.

TABLE V. DOMINANT TIDAL CONSTITUENTS

		SHELF	MOORING		SLOPE	MOORING	
	cm/s	3341 (30M)	3351 (30M)	AVG.	3461 (285M)	3462 (485M)	AVG.
K1	S.Maj.	7.642	6.782	7.212	2.195	1.876	2.035
K1	S.Min.	-3.074	-2.493	-2.78	.069	-.061	.004
K1	Inc.d.	100.9	112.1	106.5	148.9	146.3	147.6
K1	G. d.	164.8	176.6	169.7	214.7	217.4	215.8
O1	S.Maj.	3.784	3.823	3.804	1.407	1.143	1.275
O1	S.Min.	2.27	-1.497	-1.89	-.016	.017	.01
O1	Inc.d.	91.7	104.4	98.1	145.9	137.1	141.5
O1	G. d.	125.9	123.1	124.5	181	188.1	184.5
M2	S.Maj.	6.168	3.374	4.771	4.196	2.52	3.358
M2	S.Min.	1.125	1.388	1.256	-.083	1.615	.766
M2	Inc.d.	80.9	26.5	53.7	152.8	76.5	114.7
M2	G. d.	154.1	105.3	129.7	158.2	95.6	126.9
N2	S.Maj.	1.046	.896	.971	2.027	.982	1.505
N2	S.Min.	.375	.137	.256	-1.24	-.163	-.702
N2	Inc.d.	95.6	26.5	61.1	58.1	1.615	61
N2	G. d.	148.8	86.8	117.8	58.8	76.2	67.5
S2	S.Maj.	1.486	1.253	1.37	.803	1.395	1.099
S2	S.Min.	.67	.399	.535	.096	-.122	-.013
S2	Inc.d.	120.1	14.0	67.1	148.6	68.9	108.8
S2	G. d.	205	97.7	151.4	223.3	138.6	181

S.Maj. and *S.Min.* stand for semi-major and semi-minor axes of tidal ellipses in cm/s. *Inc.d.* stands for the angle measured counter-clockwise between the east axis and the semi-major axis in degrees. *G.d.* is the interval in degrees by which the instant of maximum current along the northward semi-major axis lags the simultaneous transit of the fictitious stars.

IV. HYDROGRAPHIC CONDITIONS

Hydrographic conditions in the region are presented in this chapter. Transections of temperature, salinity, density anomaly, spiciness and velocity are presented for the inshore, offshore, Farallones, and Pioneer transection. Density anomaly, gamma, is defined as

$$\gamma_\theta = \rho(S,\theta,p) - 1000 kg/m^3$$

where ρ is in-situ density, S is salinity in practical salinity units, psu, θ is potential temperature referenced to the ocean surface in degrees Celsius, and p is the pressure in decibars (UNESCO, 1987).

The state variable spiciness (π) is constructed so that its diapycnal gradient $d_\rho\pi$ is related to the density gradient ratio $R_\rho : d_\rho\pi \approx (1 + R_\rho)/(1 - R_\rho)$, where R_ρ is the ratio of the vertical gradients of temperature and salinity multiplied by the thermal expansion and saline contraction coefficients, respectively (Flament, 1986). It is a useful tracer for the description of interleaving and double diffusive processes. It is defined to be largest for warm and salty water (Flament, 1986).

All sections have been plotted at the same scale (except Pioneer section CTD plots, which are 5% smaller than the original scale). The aspect ratio (depth per unit length) is thus 4×10^{-3}.

A. INSHORE TRANSECTION

The inshore transection (Figure 3) is marked by a convergence in the velocity field at station 34. Water is moving offshore to the north of station 34 and onshore to the south of station 34. The principal feature of the salinity field is a lens of subsurface fresh water at station 36. Detailed features of individual sections are discussed below.

1. Temperature

The largest vertical temperature gradients are found in the upper 40m of the water column, and the largest temperature difference, 3C, is found at the southern end of the section at station 38. Here the water is warmest at the surface; surface temperatures cool to the north, are less than 13.5C at station 35, but warm slightly at the northern end of the transection. At 50m, the pattern is similar; temperatures are warmest to the south and coolest at the northern end of the section. Cooler water is also found below 40m at station 36.

2. Salinity

To the north of station 35, the shape of the isohalines is very similar to that of the isotherms. At station 36, a lens of fresh water, 33.25 psu, is found at about 20m. Beneath this feature, the greatest vertical salinity gradient occurs with salt increasing about .01psu/m.

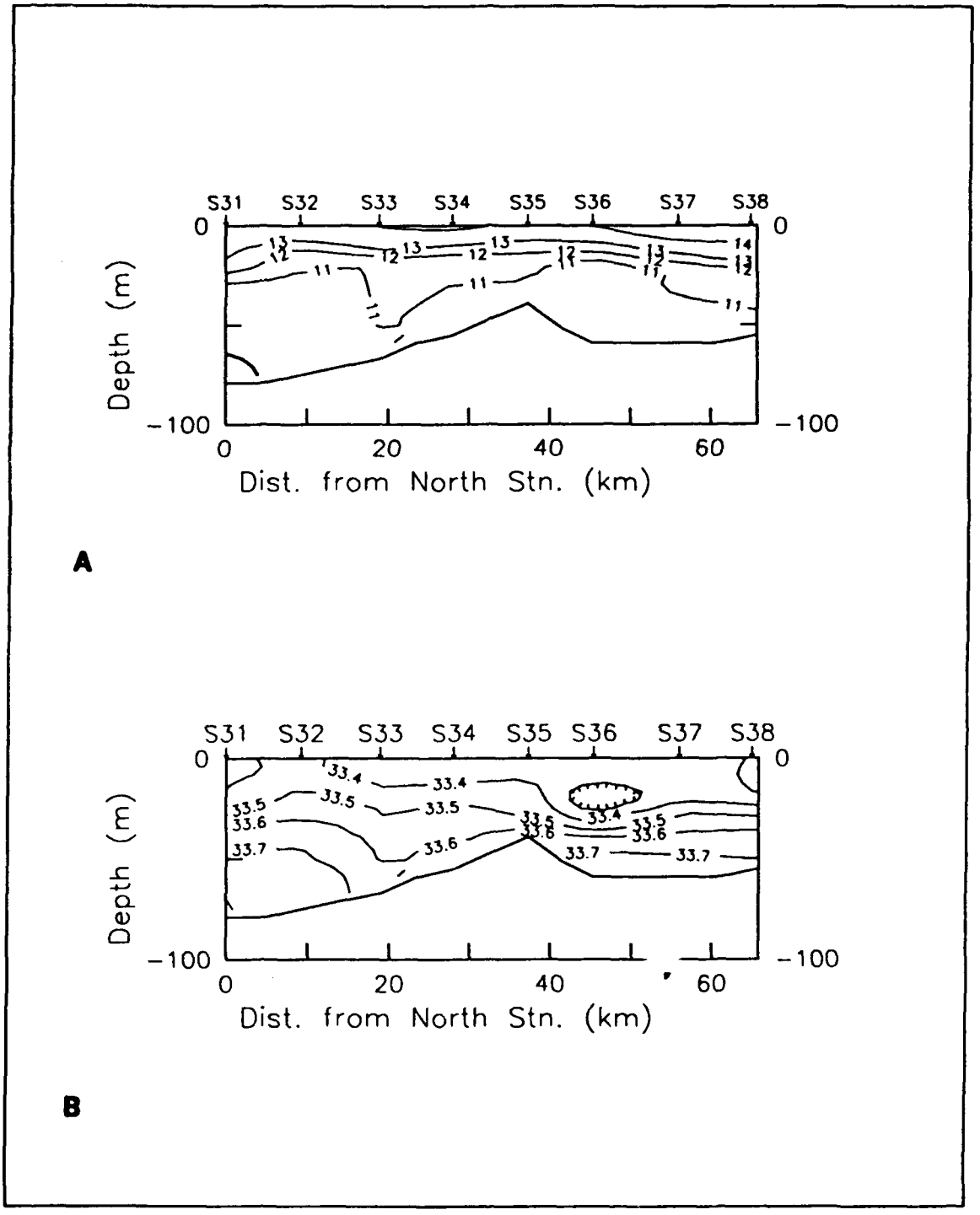

Figure 3a. Inshore Transection Temperature Field: Temperatures in °C along the Inshore Transection. CTD station locations are indicated along the top of the figure.
Figure 3b. Inshore Transection Salinity Field: Salinities in psu. Hatching indicates a minimum.

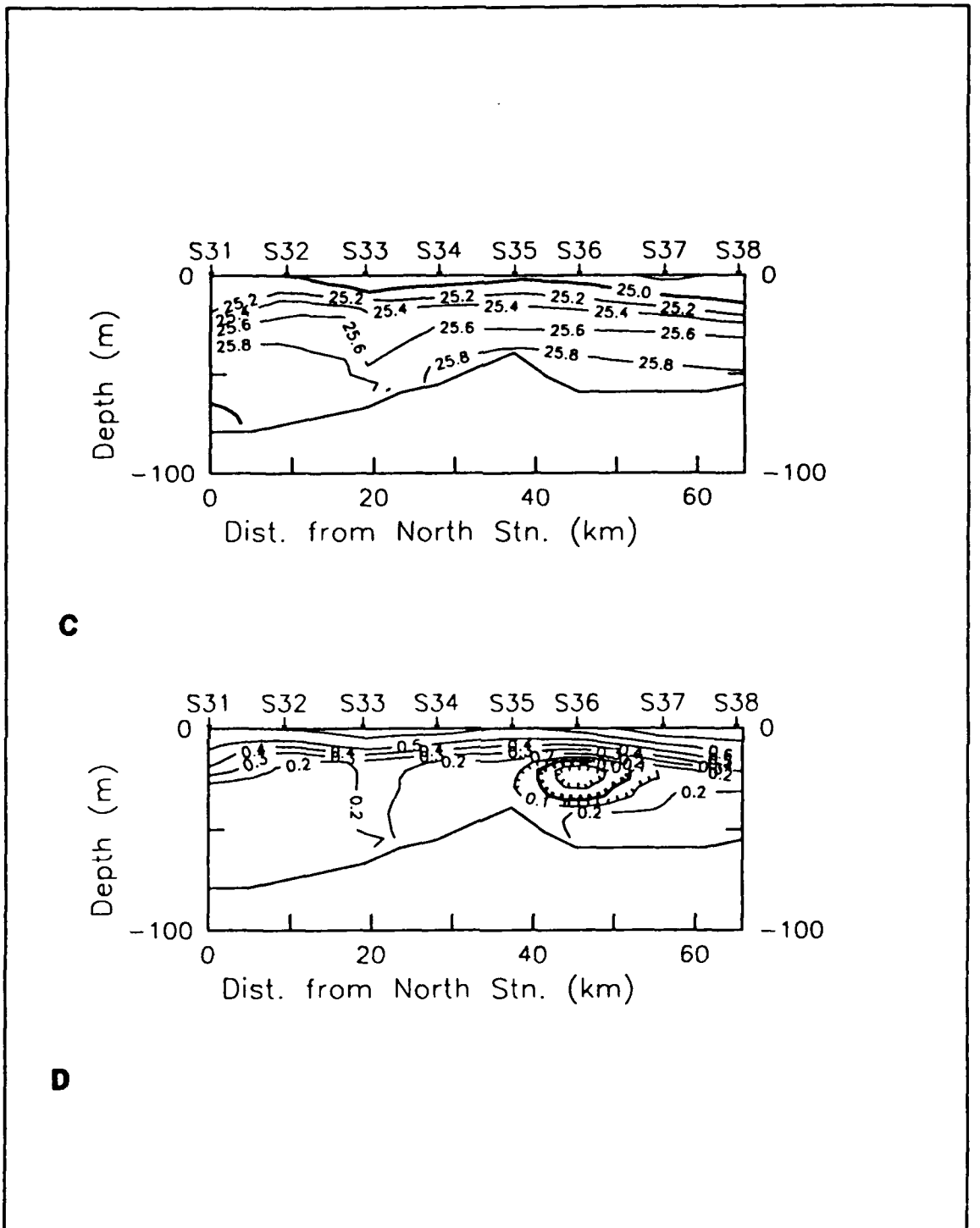

Figure 3c. Inshore Transection Density Anomaly Field: Density anomaly values in kg/m^3.
Figure 3d. Inshore Transection Spiciness Field: Hatching indicates a minimum.

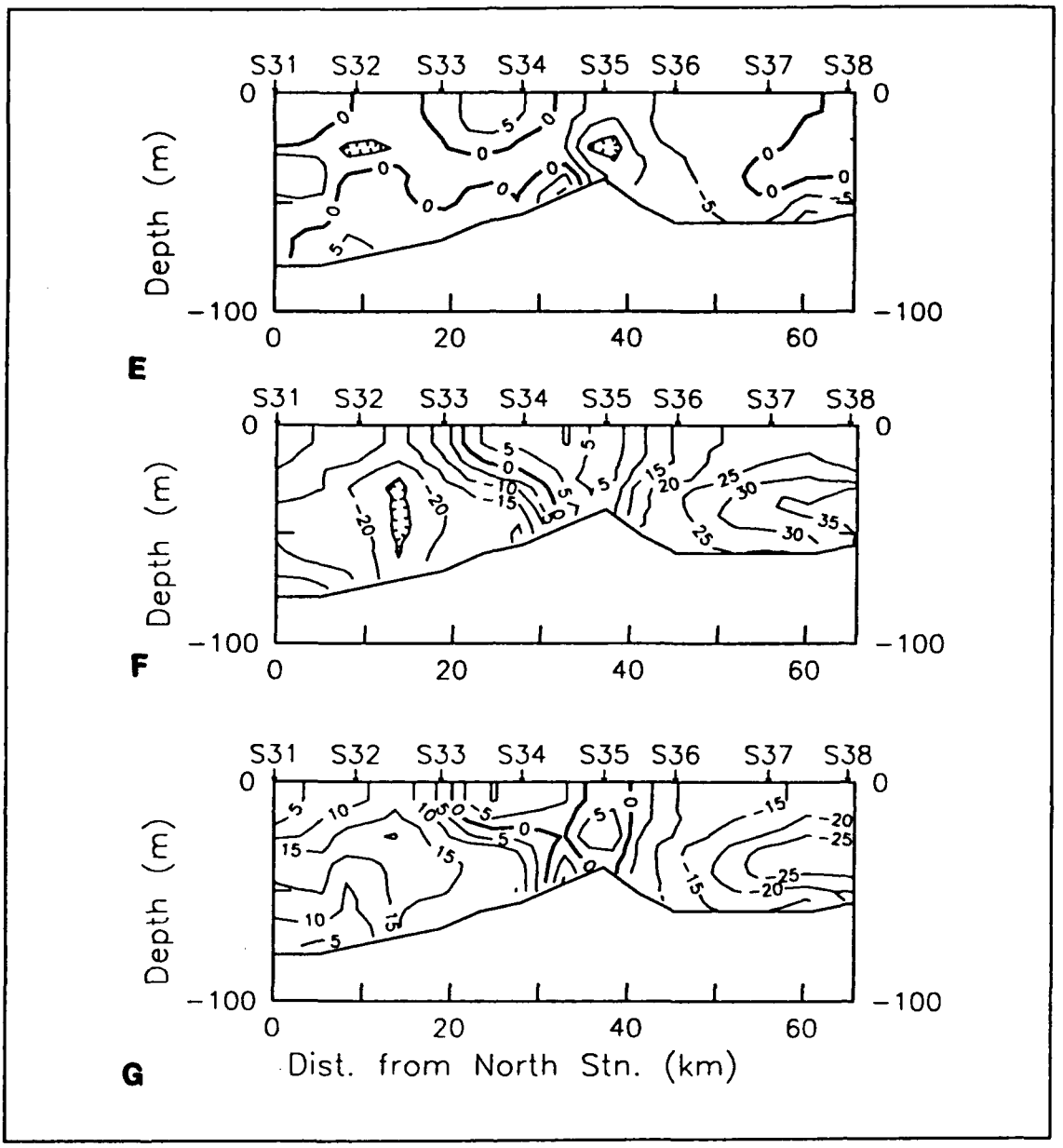

Figure 3e. Inshore Transection Detided ADCP East-West Velocity: East-west velocities in cm/s, along Inshore Transection. Positive values indicate eastward velocities. CTD Station locations are shown along the top of the figure. Hatching indicates a local minimum.

Figure 3f. Inshore Transection Detided ADCP North-South Velocity: North-south velocities in cm/s. Positive values indicate northward velocities.

Figure 3g. Inshore Transection Detided Cross Velocity: Cross-transection velocities in cm/s. Positive values indicate flow away from the coast.

To the south of station 35, isohalines of 33.65 and less shoal to the south, opposite to the slope of the isotherms.

3. Density

Since patterns of temperature and salinity were similar north of station 35, it is not surprising that the isopycnals also reflect this pattern; the pycnocline extends to the surface, and shoals at station 32. The shoaling of isotherms and deepening of isohalines associated with fresh water at station 35 appear to compensate one another in the density field; the depth of isopycnals at station 35 is about the same as station 34. South of station 35, isopycnals slope downwards toward the coast.

Although water depths are too shallow to strictly apply geostrophic principles, the pressure field should reflect the circulation patterns which can be deduced using the thermal wind relationship. This would require cyclonic circulation around station 32, and onshore flow to the south of station 36.

4. Spiciness

The most distinctive feature of the spiciness field is the minimum which corresponds to values of less than -0.1 at 35m at station 36. This feature corresponds to the salinity minimum noted above.

5. Detided East-West Velocity Field

Westward velocities dominate most of the east-west velocity section and are observed at each station. Eastward velocities are found in the upper 20m at station 31, between stations 33 and 34, and at station 38, extending to a depth of 40m at the latter station. Eastward flow at depth is observed at stations 32 to 34. The most noticable feature is a core of westward flow of -14 cm/s at station 35 (north of the spiciness anomaly at station 36). Immediately north of this velocity core, a strong horizontal shear occurs.

6. Detided North-South Velocity Field

The transition from northward to southward flow occurs between stations 33 and 34. To the south flow is northward and to the north, flow is southward. Peak speeds exceed 35 cm/s at 40m at station 38 and the largest southward flow, about 25 cm/s, was observed between station 32 and 33. Note that this implies considerable convergence of flow across the section.

7. Detided Cross-Section Velocity

Station 35 is a transition with offshore flow to the north and onshore flow to the south, although flow above 20m at station 34 is onshore as well. Peak onshore velocities of 25 cm/s were observed at 35m at station 38 and peak offshore velocities of 20 cm/s were observed at 25m at station 32.

B. OFFSHORE TRANSECTION

A subsurface salinity minimum (Figure 4) is found at stations 9 and 10 at about the same depth and to the west of that observed in the inshore section. Flow patterns are also similar; a shear zone occurs between stations 10 and 11 with westward flow to the north and eastward flow between stations 7 and 10. In this section, strong convergence does not occur at the shear zone.

1. Temperature

The mixed layer for this transection is 20m or less. Surface temperatures decrease to the south. The upper 50m is strongly stratified, with the temperature change decreasing from 4C at station 15 at the northern end of the section to 2.5C at station 1 at the southern end of the section. Several wave-like features appear in the upper 50m; proceeding from north to south, isotherms shoal to station 9, deepen at station 7, shoal at station 5, deepen at station 3 or 4, and shoal again at station 1. These features are probably due to internal waves.

Below 200m, water appears to be about 0.5C cooler at station 13 than stations 3 and 4.

The slope of upper ocean isotherms are not always indicative of the slope of subsurface isotherms. Between Stations 14 and 11, the 10C isotherm deepens while those above shoal. This isotherm also deepens at station 5 while shallower

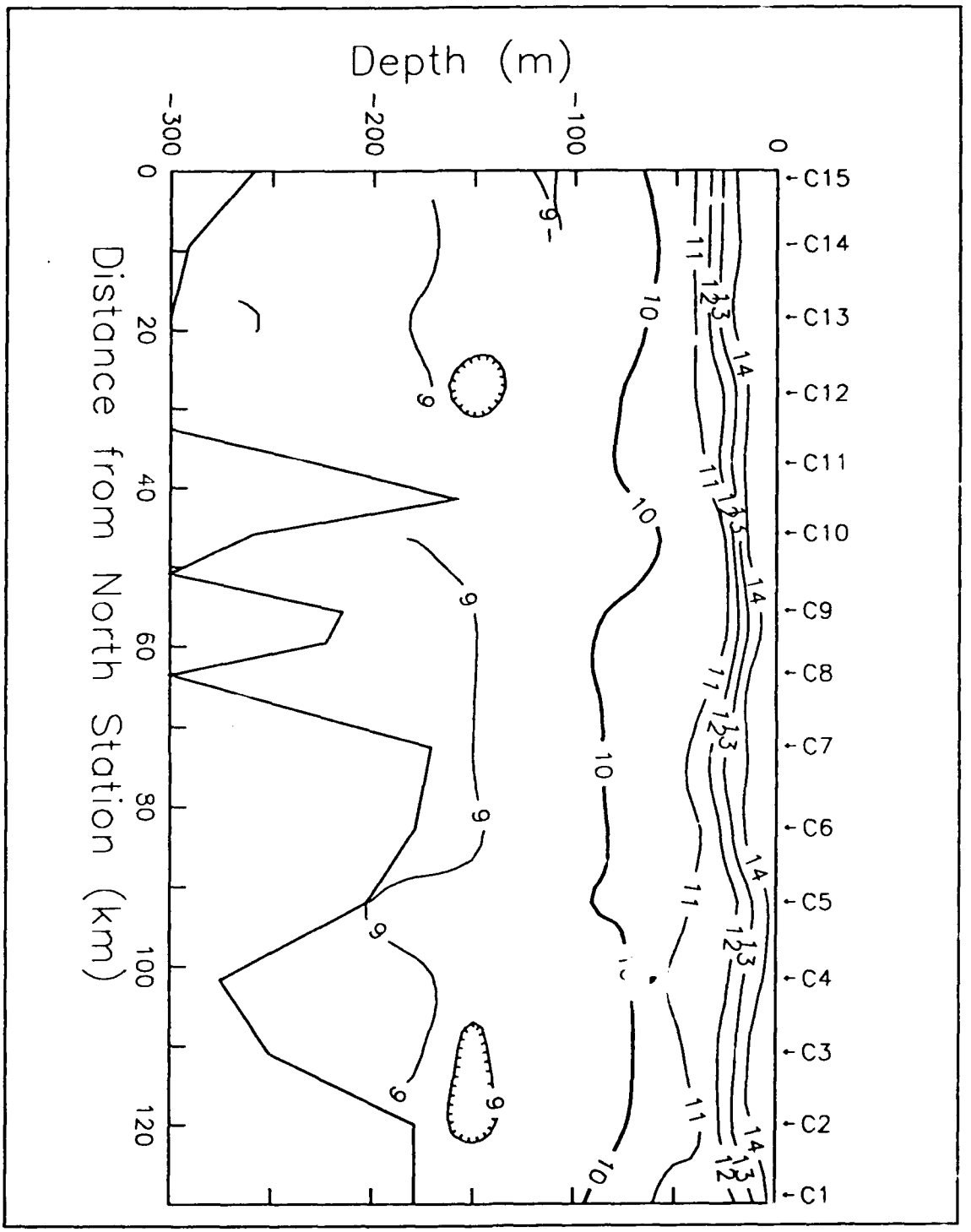

Figure 4a. Offshore Transection Temperature Field: Temperatures in °C along the Offshore Transection. CTD station locations are indicated along the top of the figure. Hatching indicates a minimum.

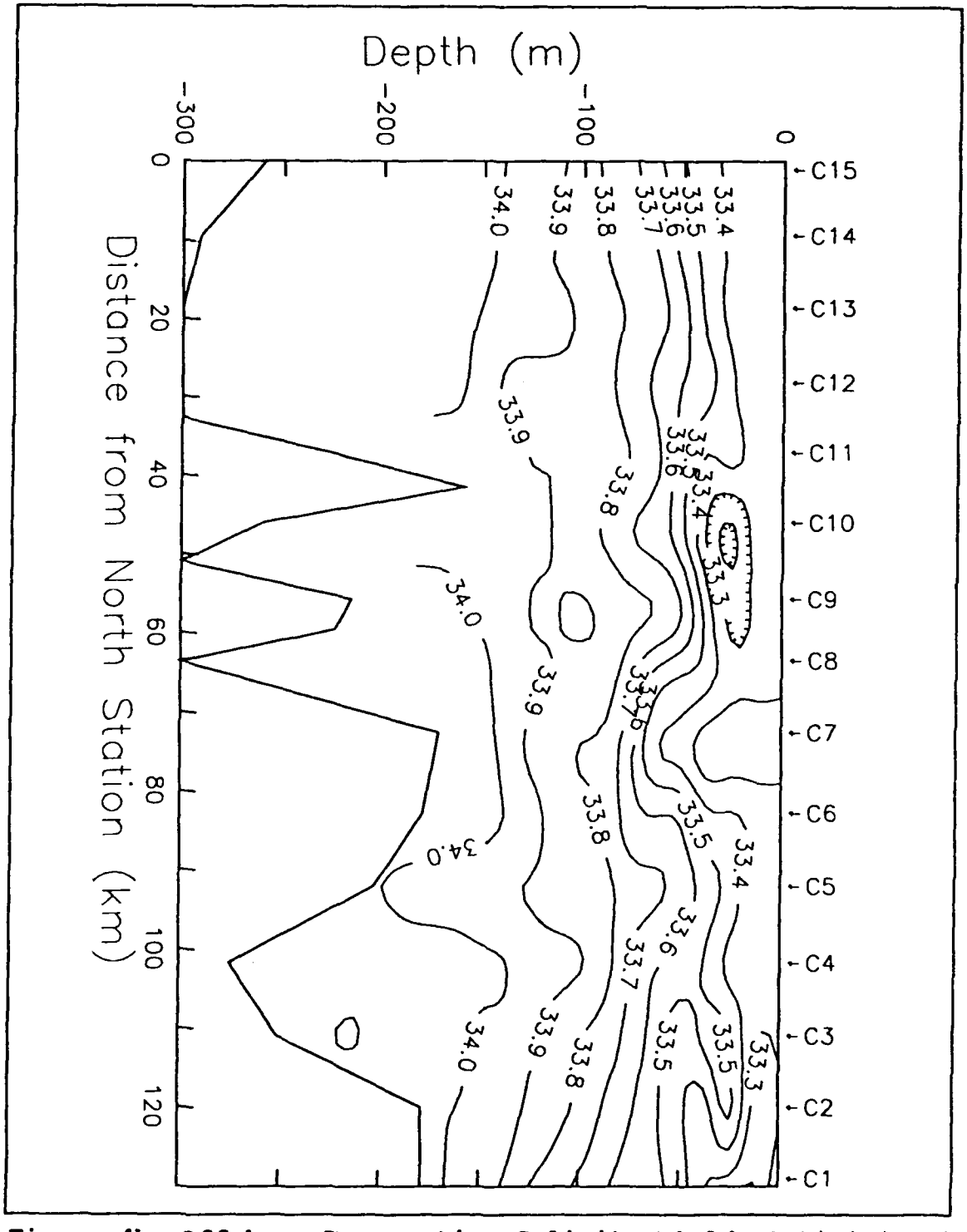

Figure 4b. Offshore Transection Salinity Field: Salinities in psu along the Offshore Transection. CTD station locations are indicated along the top of the figure. Hatching indicates a minimum.

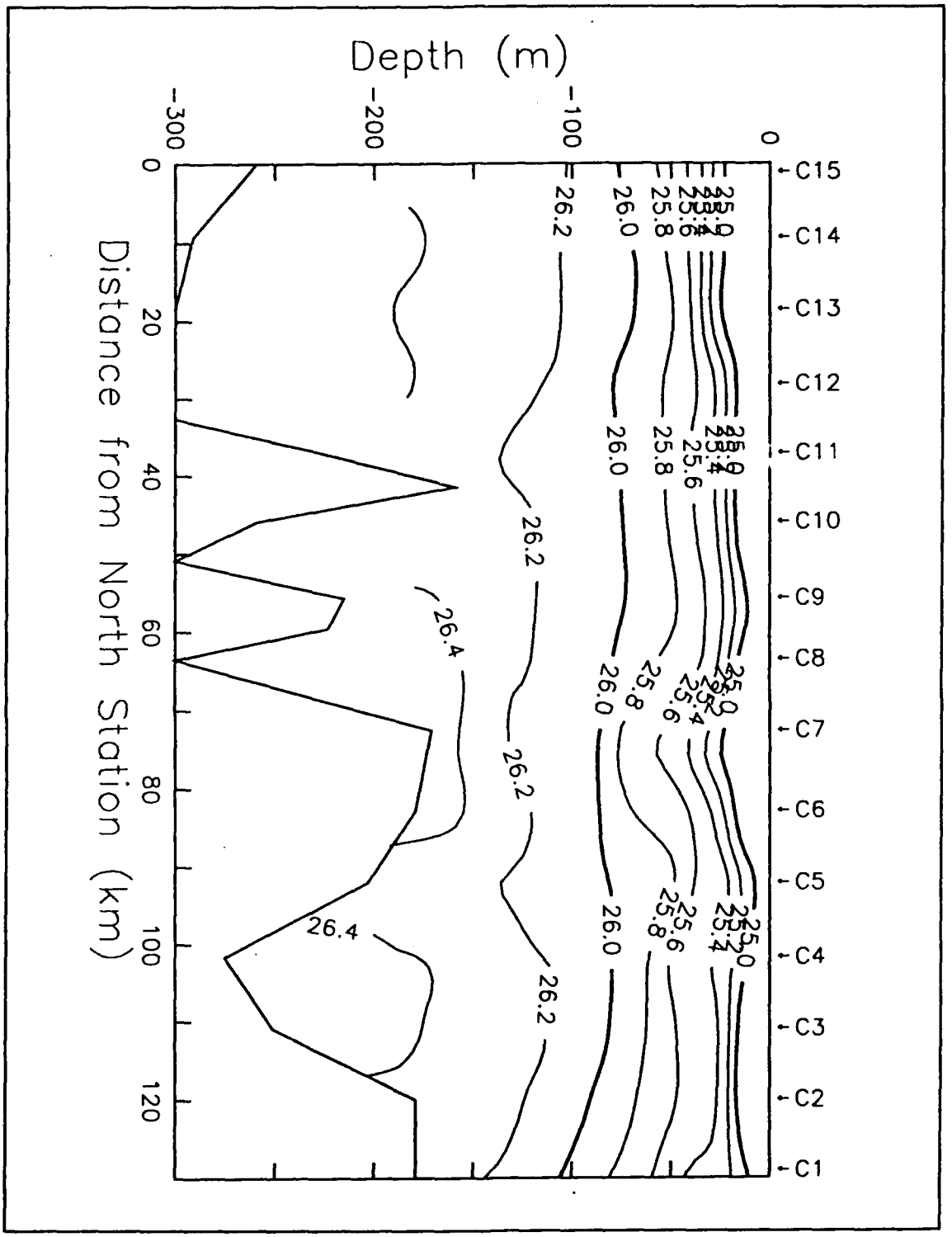

Figure 4c. Offshore Transection Density Anomaly Field: Density anomaly values in kg/m^3 along the Offshore Transection. CTD station locations are indicated along the top of the figure.

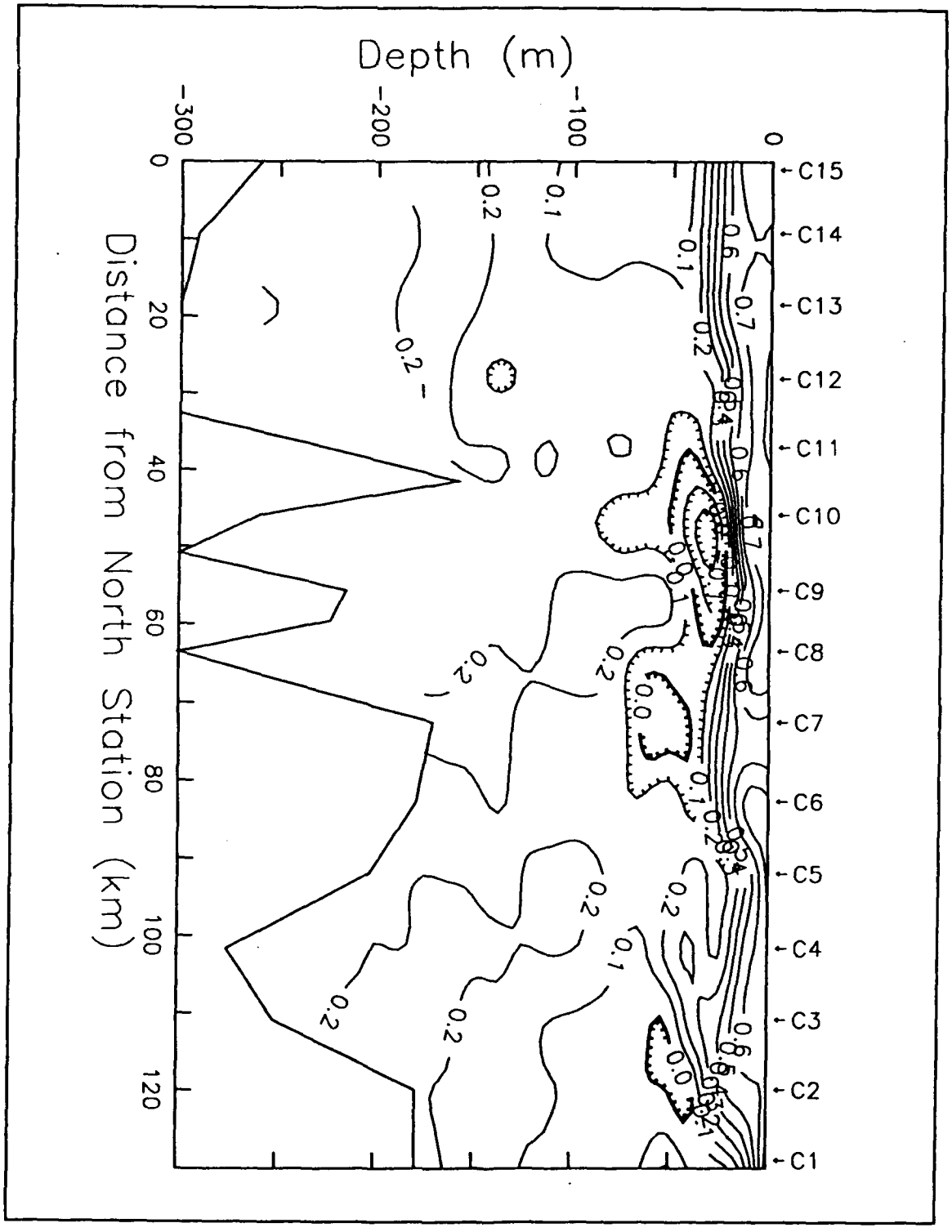

Figure 4d. Offshore Transection Spiciness Field: Spiciness values along the Offshore Transection. CTD station locations are indicated along the top of the figure. Hatching indicates a minimum.

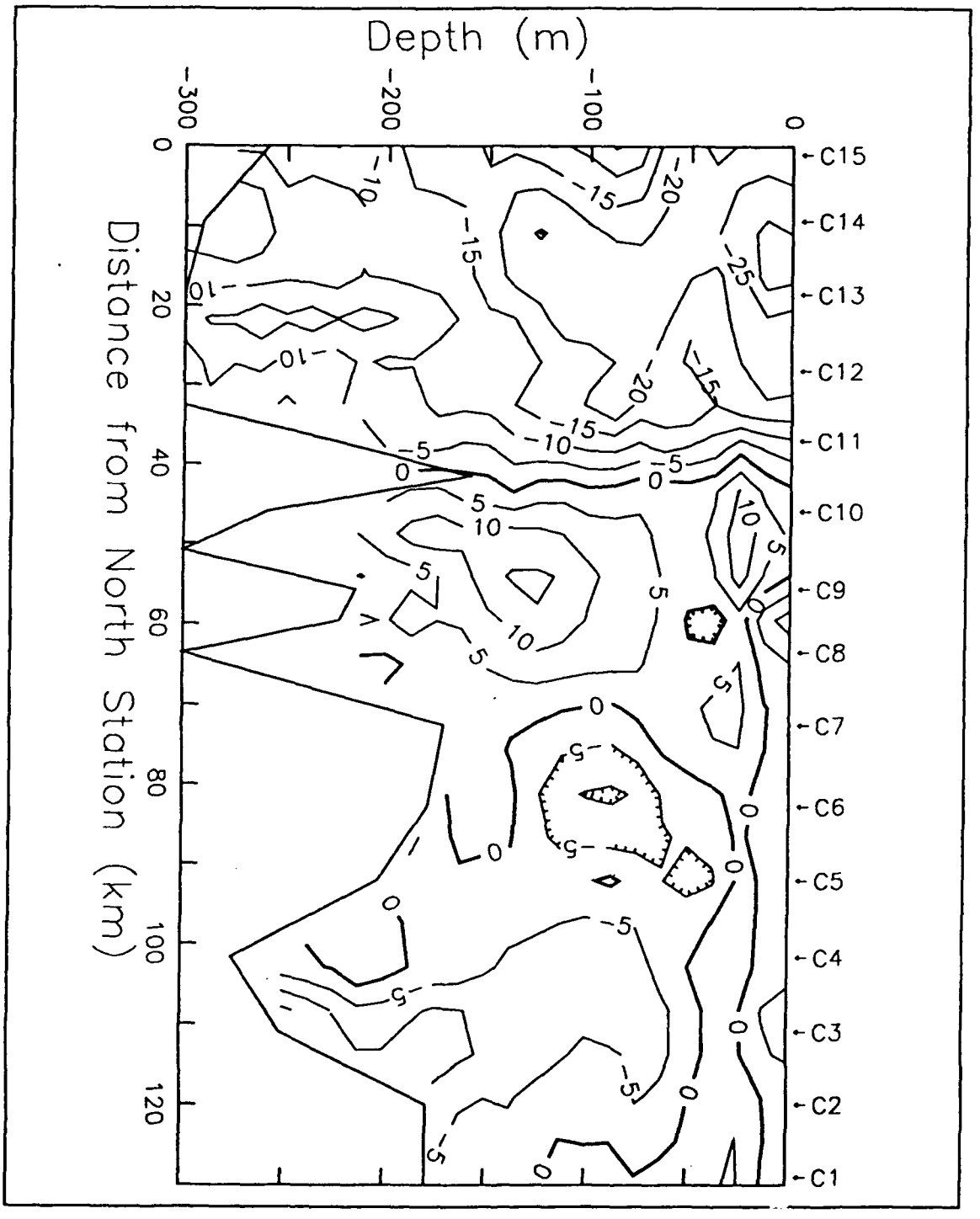

Figure 4e. Offshore Transection Detided ADCP East-West Velocity: East-west velocities in cm/s along the Offshore Transection. Positive values indicate eastward velocities. CTD station locations are shown along the top of the figure. Hatching indicates a minimum.

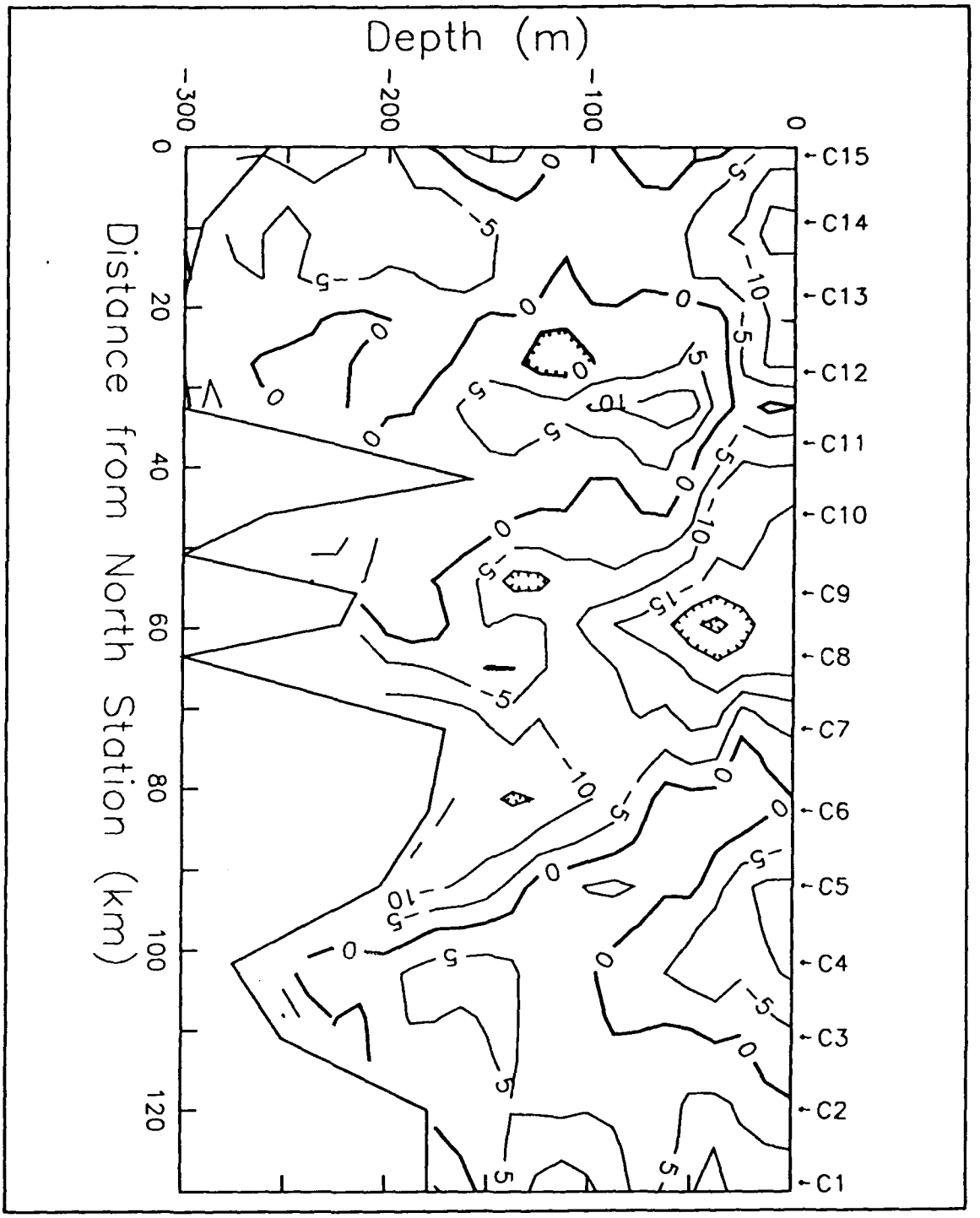

Figure 4f. Offshore Transection Detided ADCP North-South Velocity: North-south velocities in cm/s along the Offshore Transection. Positive values indicate northward velocities. CTD station locations are shown along the top of the figure. Hatching indicates a minimum.

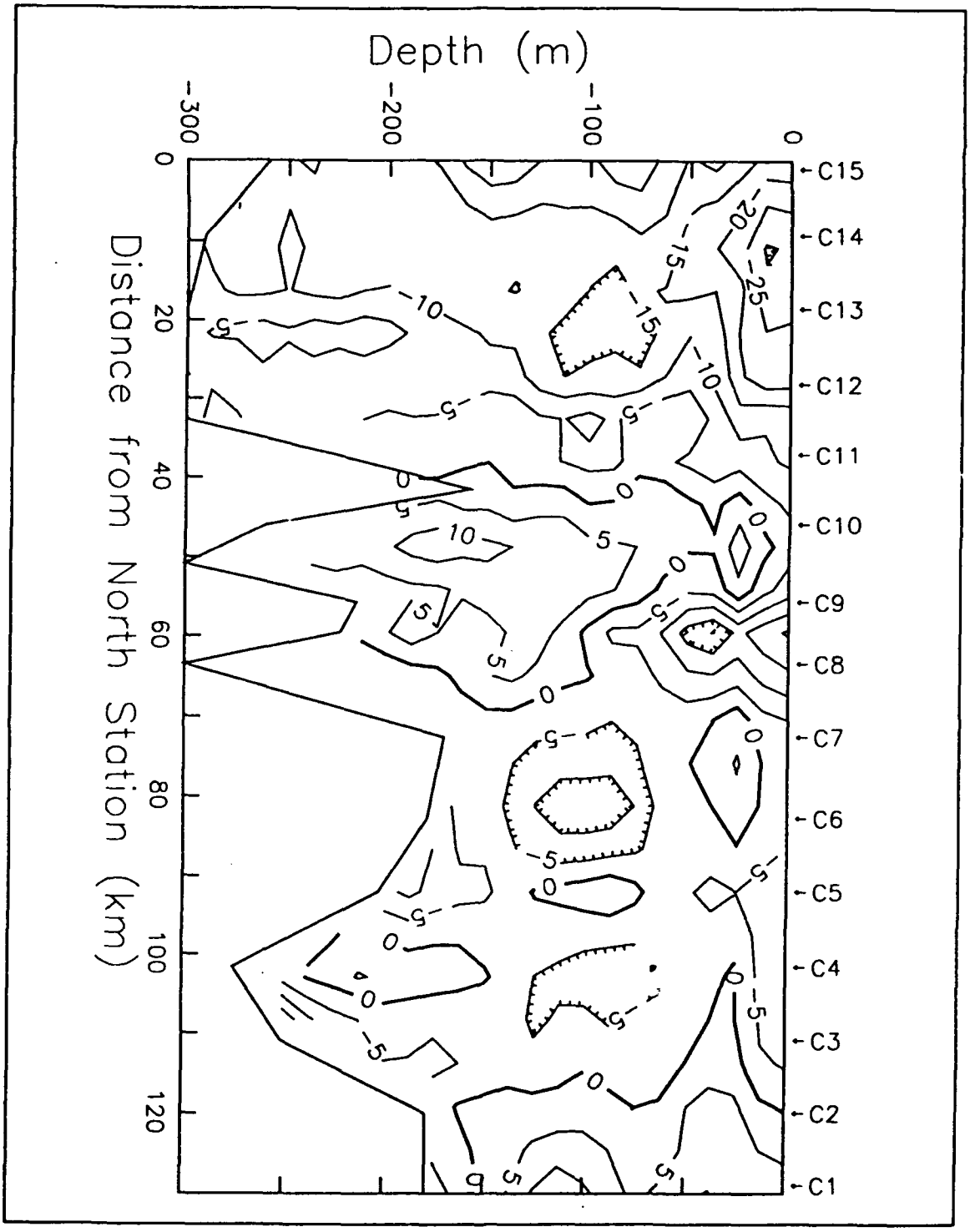

Figure 4g. Offshore Transection Detided ADCP Cross Velocity: Cross-transection velocities in cm/s along the Offshore Transection. CTD station locations are shown across the top of the figure. Hatching indicates a minimum. Positive values indicate flow toward the coast.

isotherms shoal. Finally, at station 1, isotherms below 11C deepen to the south while those shallower shoal.

2. Salinity

The saltiest water at the surface was observed at stations 5 and 6, 33.39 psu; the freshest water was observed at station 7, 33.24 psu. Subsurface, strong stratification is not found in the upper 50m as was the case with temperature. Instead, the strongest salinity stratification is found between 40 and 100m; at station 15, the salinity change in this interval is 0.45psu and at station 1 the change is 0.35 psu.

Wave-like features, similar to the temperature section, are seen again. These are associated with 33.3psu (fresh) features at station 10, 7, and 1. The feature at station 7 corresponds to a trough in the upper temperature field, and the core of fresh water at station 10 corresponds to the fresh water core with 33.3 psu at station 36 of the inshore transection.

At the southern end of the section, isohalines slope downward to the south from station 5 or 4 to the end of the section. Note that the isotherms behave differently, sloping in a similar manner only below 40 or 50m and from station 3 or 2.

3. Density

The features seen in the temperature and salinity sections appear somewhat smoothed in the density section. Strongest stratification occurs in the northern part of the section and the wave-like features in the upper 60m correspond to isotherm features.

The 25.0 through 25.4 isopycnals shoal to the south, while below 50m, beginning with the 25.8 isopycnal, isopycnals slope downward. From the north end of the transect to station 9, isopycnals are relatively smooth and parallel to one another for the upper 80m. From station 9 south to station 7, they slope down sharply, and from station 7 south to station 5, they slope upward again. With the thermal wind relationship, this requires an onshore transport betwen stations 9 and 7, and offshore transport between stations 7 and 5. Using the same argument, from station 3 to the south end of the transect, isopycnals slope down below 30m, indicating onshore transport for this portion of the transection.

4. Spiciness

A spiciness minimum is centered at 50m at station 10. This corresponds to the salinity minimum noted above. Spiciness minima also occur at stations 7 and 2.

A vertical gradient in spiciness occurs in the upper 50m. Except for the spiciness minimum, subsurface spiciness is

quite uniform, greater than 0 and less than 0.3. At stations 6 and 12, the spiciness is even more uniform, between 0.1 and 0.2. Values greater than 0.2 below 100m are associated with the upper portion of California Undercurrent waters (see below). The alongshore distribution of these features (stations 4, 8, 11 to 15) is not uniform.

5. Detided East-West Velocity

The pattern of the east-west velocity field is one of westward flow to the south of station 7 and to the north of station 10 with eastward velocity in between, although a core of eastward flow is also found at 30m at stations 1 to 5. The largest velocities are at the surface at stations 13 and 14, about 30 cm/s, and this strong flow, as indicated by the 20 cm/s isotach, extends to 150m at these stations. The strongest eastward flows are at a depth of 150m at station 9, about 15 cm/s. Note that the low spiciness, fresh water at station 10, is moving eastward.

6. Detided North-South Velocity

Southward flow occurs at the surface to the north of station 2 and subsurface also dominates the section. Northward flow is at the southern end of the section, extending as a tongue almost to the surface at station 6. Northward flow is also found subsurface at stations 10 to 12 and 15. Largest northward velocities of 10 cm/s are found at 70m at station

12; largest southward velocities, 25 cm/s, are found at 40m at station 9.

7. Detided Cross-section Velocity

Because of the orientation of the section along 325 degrees, both components of velocity are weighted equally in computing the cross-section velocity. Offshore flow is found at the surface to the north of station 2, and also fills most of the volume subsurface as well. The major exception is the region between stations 10 to 8 where onshore flow is found. Largest offshore velocities are found at the surface, about 30 cm/s, and maximum onshore velocities were observed at station 1, and 9, in excess of 10 cm/s.

C. FARALLONES TRANSECTION

Poleward flow (Figure 5) appears as a wedge which penetrates upward from a depth of 400m at 40km from shore to the surface at 65 km from shore with strongest flow at the surface over the shelf break. The east-west field is marked by a band of westward flow which diverges from the slope. Salinity inversions were not observed in the upper 100m; below this depth, warmer, saltier waters of equatorial origin appear to the west of station 60.

1. Temperature

There is a strong vertical temperature gradient in the upper 50m of the water column with temperature changes as great as 0.1C/m. At the surface, waters are coolest in the

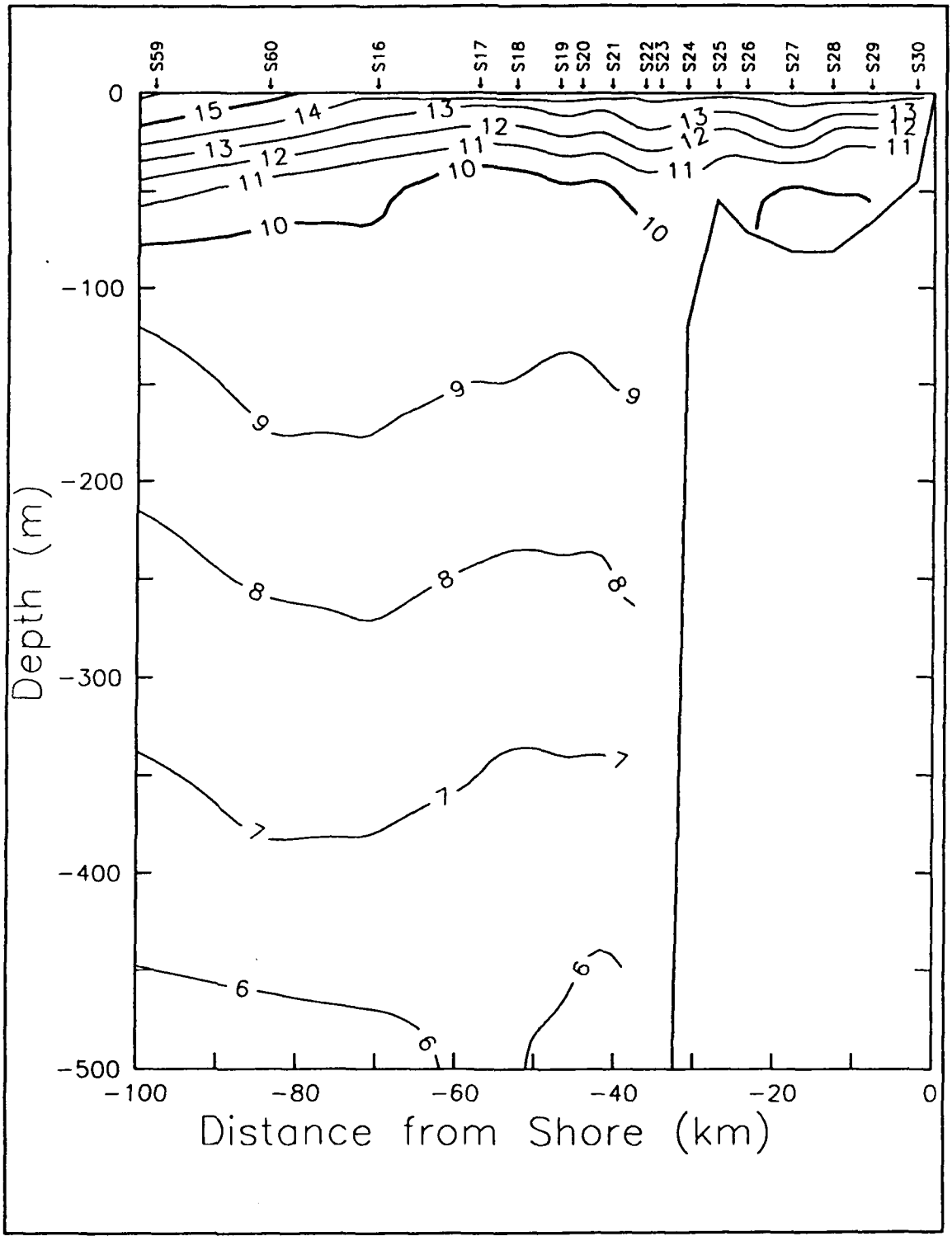

Figure 5a. Farallones Transection Temperature Field: Temperatures in °C along the Farallones Transection. CTD station locations are indicated along the top of the figure.

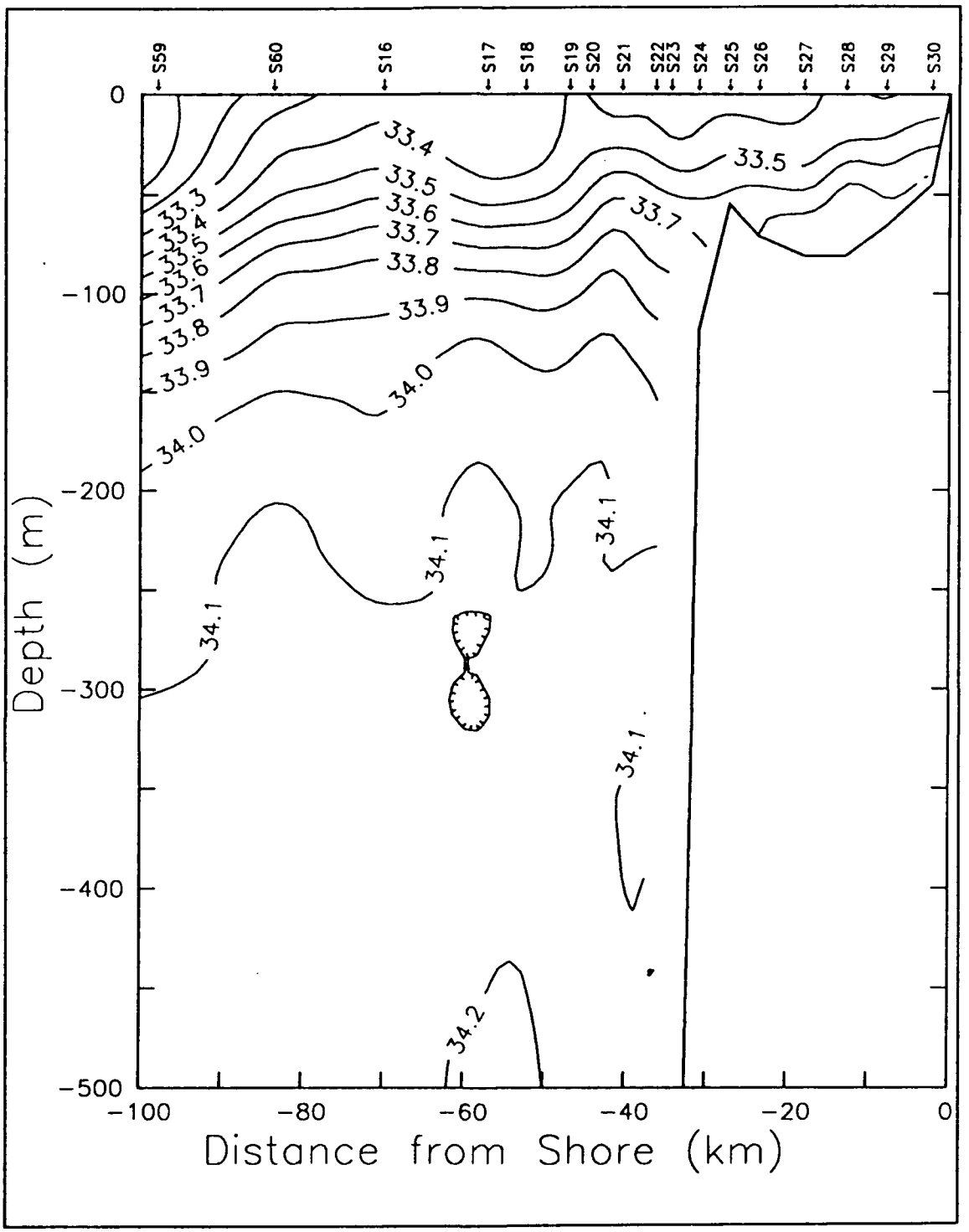

Figure 5b. Farallones Transection Salinity Field: Salinities in psu along the Farallones Transection. CTD station locations are indicated along the top of the figure. Hatching indicates a minimum.

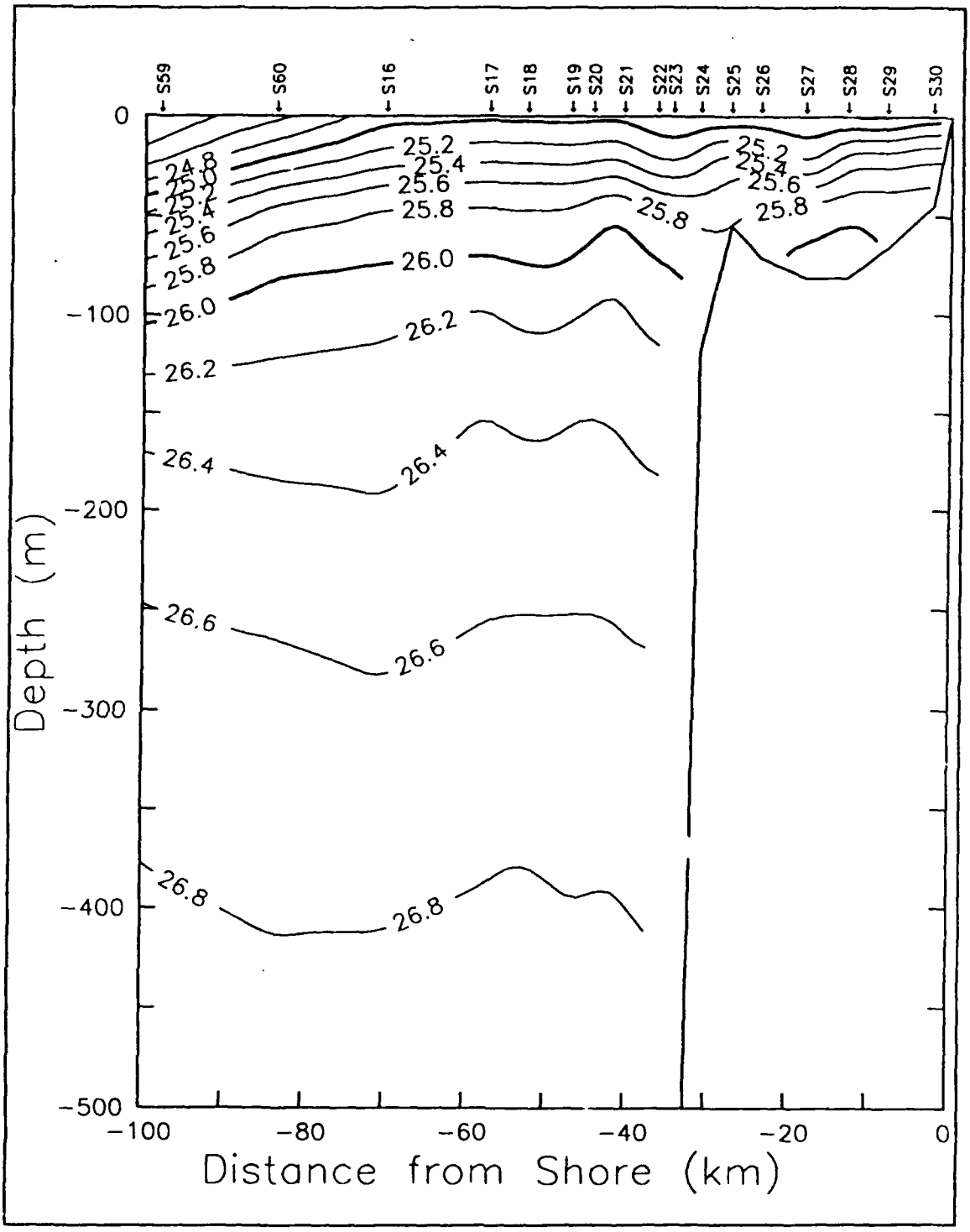

Figure 5c. Farallones Transection Density Anomaly Field: Density anomaly values in kg/m^3 along the Farallones Transection. CTD station locations are indicated along the top of the figure.

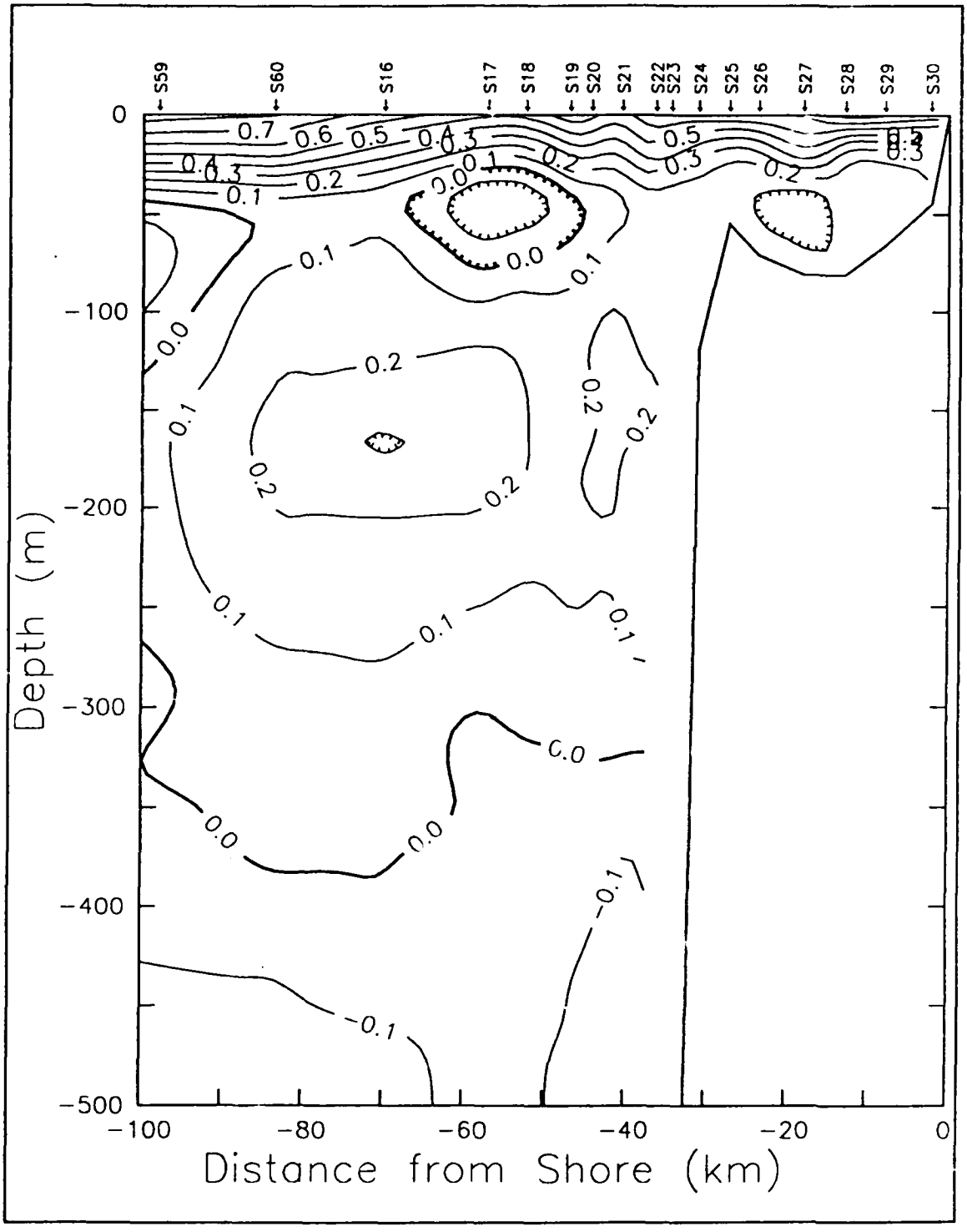

Figure 5d. Farallones Transection Spiciness Field: Spiciness values along the Farallones Transection. CTD station locations are indicated along the top of the figure. Hatching indicates a minimum.

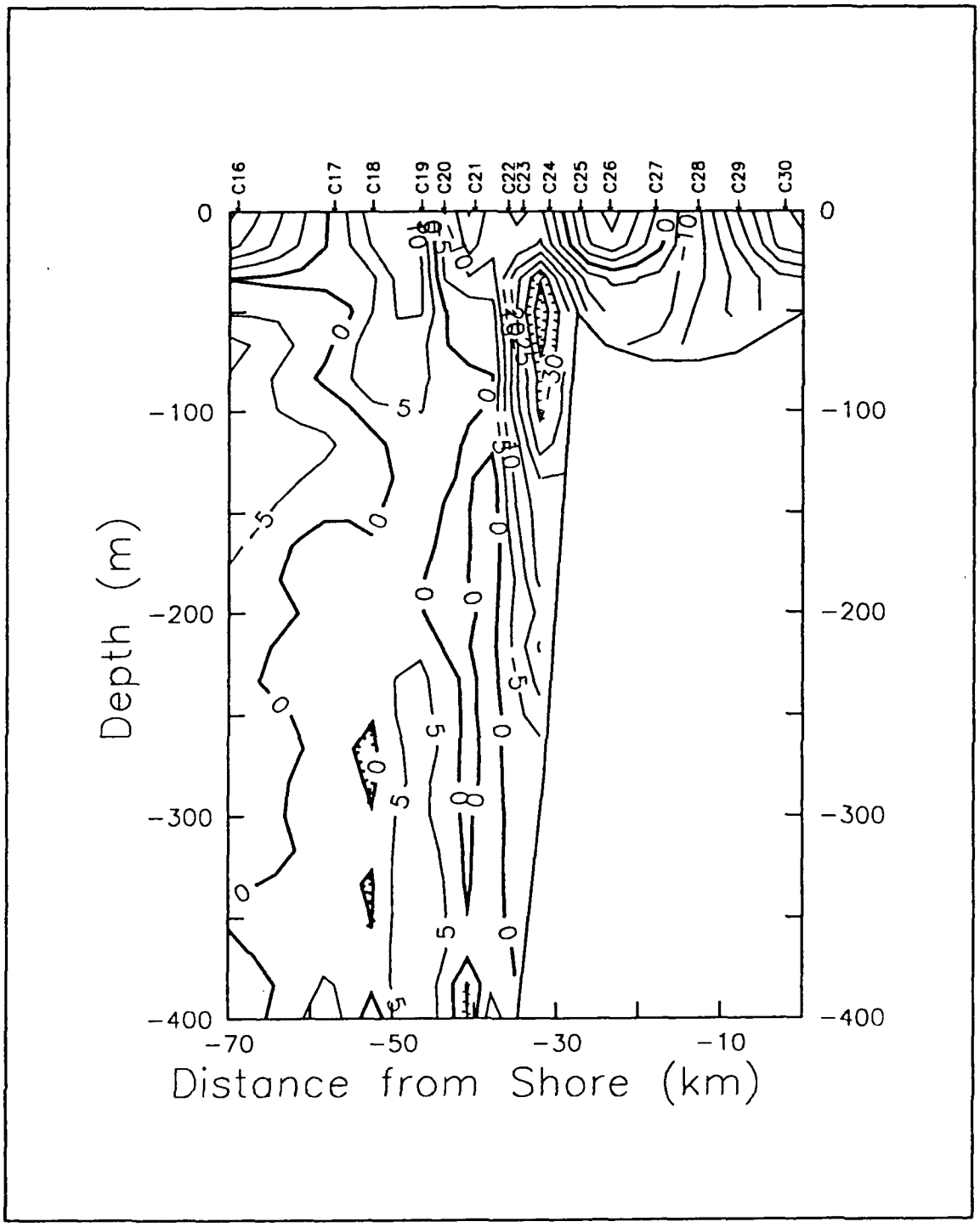

Figure 5e. Farallones Transection Detided ADCP East-West Velocity: East-west velocities in cm/s along the Farallones Transection. Positive values indicate eastward velocities. CTD station locations are shown along the top of the figure. Hatching indicates a minimum.

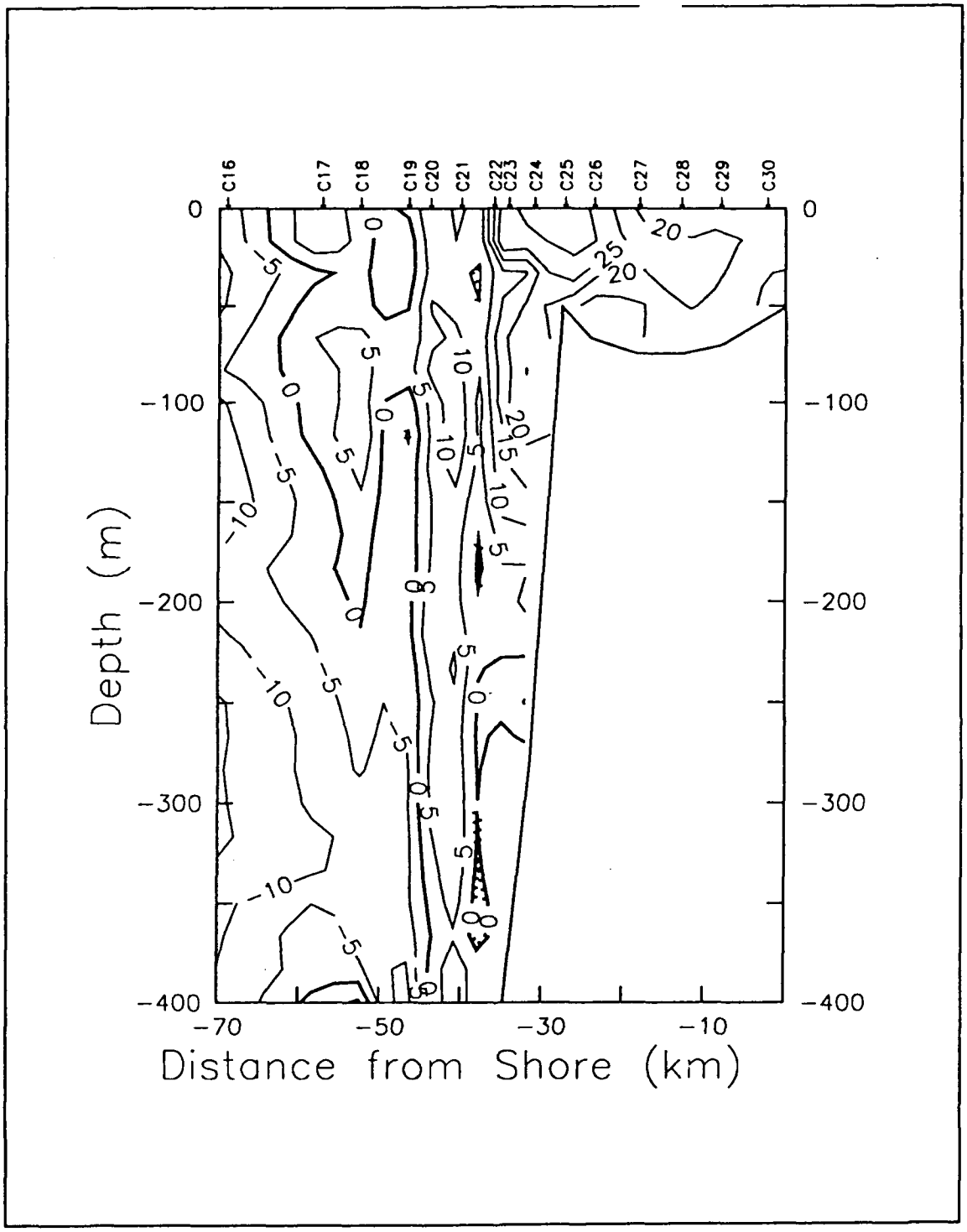

Figure 5f. Farallones Transection Detided ADCP North-South Velocity: North-south velocities in cm/s along the Farallones Transection. Positive values indicate northward velocities. CTD station locations are shown along the top of the figure. Hatching indicates a minimum.

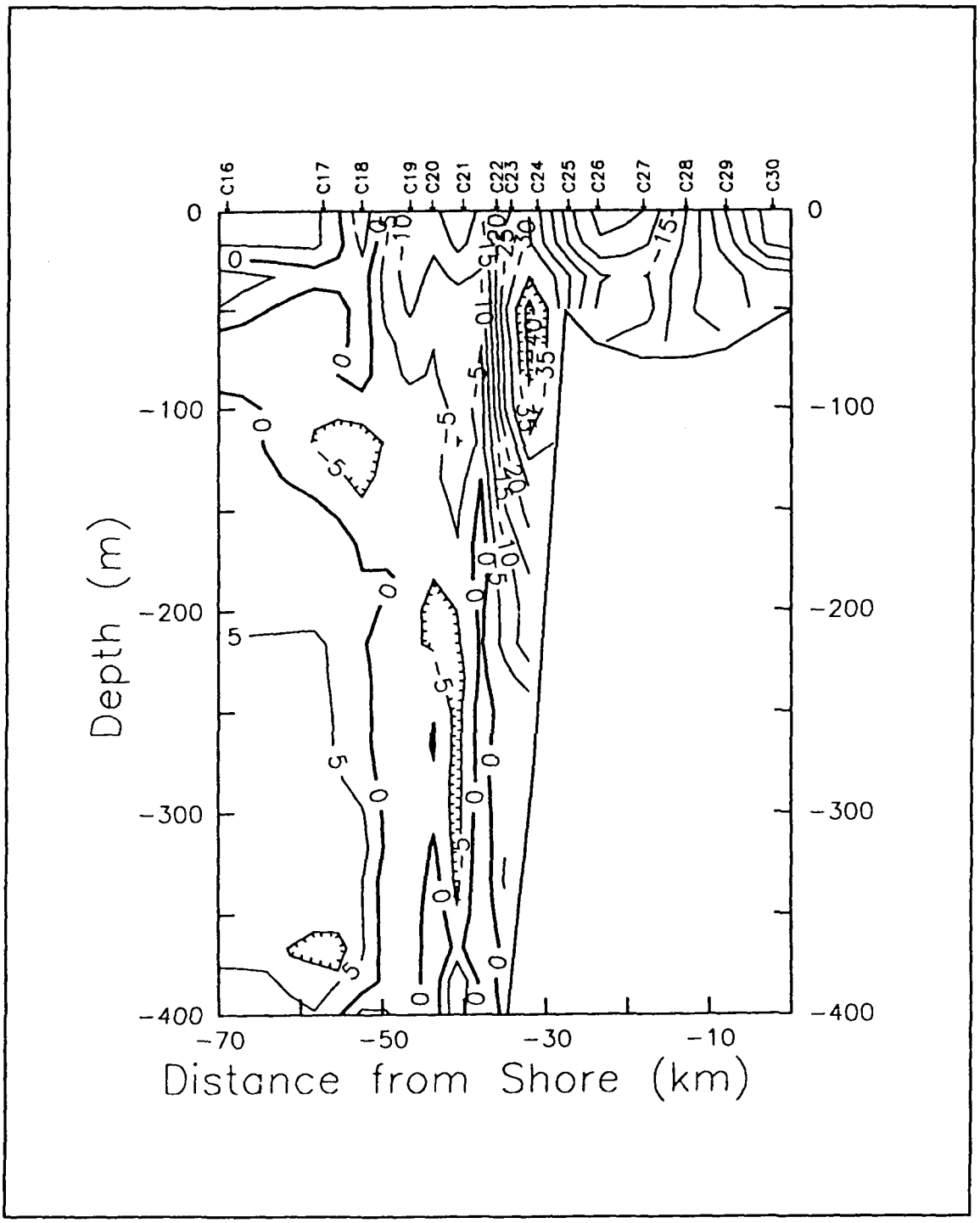

Figure 5g. Farallones Transection Detided ADCP Cross Velocity: Cross-transection velocities in cm/s along the Farallones Transection. Positive values indicate south-eastward flow. CTD station locations are shown along the top of the figure. Hatching indicates a minimum.

middle of the section, 14.3C at station 26, warmest farthest from shore, 16.4C at station 59, but temperatures of 14.9C are also found at stations 28 and 29 in the Gulf. In the upper 80m, isotherms slope upward toward shore from Station 59 to station 17 or 18, thence slope downward toward the shelf break; over the shelf break, isotherms have a wave-like pattern (probably due to internal wave activity), and thence are level over the inner Gulf.

The doming of isotherms which occurs at station 17 or 18 in the upper 80m, migrates inshore to stations 20 and 21 at depth. Unlike the upper layer, a trough is also seen subsurface, occurring at stations 60 and 16 at 9C.

2. Salinity

Near the surface, water freshens as we move offshore. At the surface, the freshest water was observed at the station farthest from shore, 33.05 psu, and the saltiest water was observed at the coast, 33.44 psu. In fact, between station 16 and the coast, the surface salinity was remarkably uniform, ranging from 33.31 psu to 33.46 psu. Subsurface salinity inversions, seen on previous sections, do not appear.

Over the continental shelf, the isohalines slope upward toward the coast. Surface and bottom layers appear well mixed, the former about 33.45 psu and the latter 33.7 psu.

Subsurface, isohalines seaward of the shelf break typically have slopes which are opposite to those of

isotherms, reflecting the transition from Subarctic water offshore to Equatorial water inshore. In general, isohalines slope upwards toward the coast, reflecting the saltier water which is usually found inshore. But at station 21, the isohalines slope downward and intersect the slope so that fresher waters are actually found within 10 km of the slope. Note the thick layer of more or less constant salinity between 34.1 and 34.2 psu.

The wave pattern which was evident subsurface in the temperature section is somewhat harder to see in the salinity section, in part due to the fact that salinity changes little beneath 200m. A careful inspection indicates that between stations 59 and 20, the patterns are inverse (troughs in isohalines corresponding to crests in isotherms) as expected. Inshore of station 20, this pattern breaks down, and slopes are similar.

3. Density

The isopycnals are similar in pattern to isotherms. In surface waters the density anomaly is less than 25 kg/m^3, and are remarkably uniform inshore of station 16. In the upper 50m, isopycnals slope upward toward the coast, except for wave-like "w" over the slope and outer shelf. Beneath 150m, isopycnals downwell from station 59 to 16, then upwell to station 20, and thence slope down toward the slope, the latter feature similar to the shape of the upper ocean isopycnals.

The thermal wind relationship requires a cyclonic shear associated with the doming of the isopycnals. Studies off Pt. Sur (Robson, 1990) have shown that the downwelling isopycnals at the slope corresponds to poleward currents.

4. Spiciness

Subsurface, large positive values of spiciness are associated with the Equatorial waters which have been transported poleward by the California Undercurrent. These waters are clearly evident between 100 and 250m from the slope to a distance 85 km from shore. Below 50m, the largest values of spiciness were found at 150m at station 21, 0.216. The negative spiciness at 50m at stations 17 and 18 represents a different water mass than that associated with waters on the shelf at stations 10 and 36, based on the temperature and salinity characteristics at each site.

5. Detided ADCP East-West Velocity

Velocity measurements between stations 60 and 16 are not included because they were observed about 85 hours after station 16 was occupied. Westward velocities dominate the 35km of the section which are closest to shore. At Pt. Reyes, the westward flow exceeds 40 cm/s. A nearshore lens of eastward flow occurs at station 26, so that a convergence of the flow field occurs inshore and divergence over the shelf break. Isotachs indicate that the westward flow also exceeds 40 cm/s between station 23 and 24 at a depth of 55m.

Weak eastward velocities predominate between station 17 and 22 and westward velocities occurred between 40 and 350m at station 16.

6. Detided ADCP North-South Velocity

The inshore 45km of this section is dominated by northward flow. Strongest velocities, 30 cm/s, are found at the shelf break, and velocities over the shelf exceed 20 cm/s. A core of northward flow was also found at station 21, corresponding to the maximum noted above. Offshore of station 19, equatorward flow dominates the section, with the strongest flow, 15 cm/s, occuring at a depth of 300m at station 16.

7. Detided ADCP Cross-section Velocity

Since the Farallones transection ran along a northeasterly course, velocities have been rotated so that negative isotachs correspond to northwestward flow and positive isotachs are southeastward flow. Since northward and westward components of flow dominate inshore, it is not surprising that this is reflected in this rotated section; isotachs indicated speeds exceeding 40 cm/s at the surface at Pt. Reyes and at 55m between station 23 and 24. On the shelf, this northwestward flow is a minimum at the surface at stations 26 and 27.

Offshore of station 22, northwestward flows weaken considerably. Southeastward flow dominates only the area below 150m and farther than 50km from shore.

D. PIONEER TRANSECTION

The Pioneer transection (Figure 6) shares station 59 with the Farallones transection. Stations 55 and 56 occur over the top of Pioneer seamount where water depth is about 1000m.

The velocity field is marked by a strong divergence at station 49, and by a weak northward flow over most of the section. The signature of the Undercurrent (warm, salty water at depth inshore and isopycnals which slope downward into the slope) is stronger in this section than the Farallones section. Shallow salinity inversions are common along this section, some of which are associated with fresher surface waters found offshore.

1. Temperature

As with other sections, the upper 50m shows strong vertical stratification. Warmest sea surface temperatures were observed at station 59, 16.4C; surface temperatures cool toward the coast, with a minimum observed at station 44, 14.4C, and thence warm, reaching a temperature of 15.0C at the coast (station 39). These upper ocean isotherms shoal from station 59 through station 47, thence sink across the upper slope, shelf break, and outer shelf to station 44, then upwelling across the midshelf, before sinking again at the coast.

Below about 100m, isotherms have a different pattern, sinking toward the coast. For example, the 8C isotherm sinks

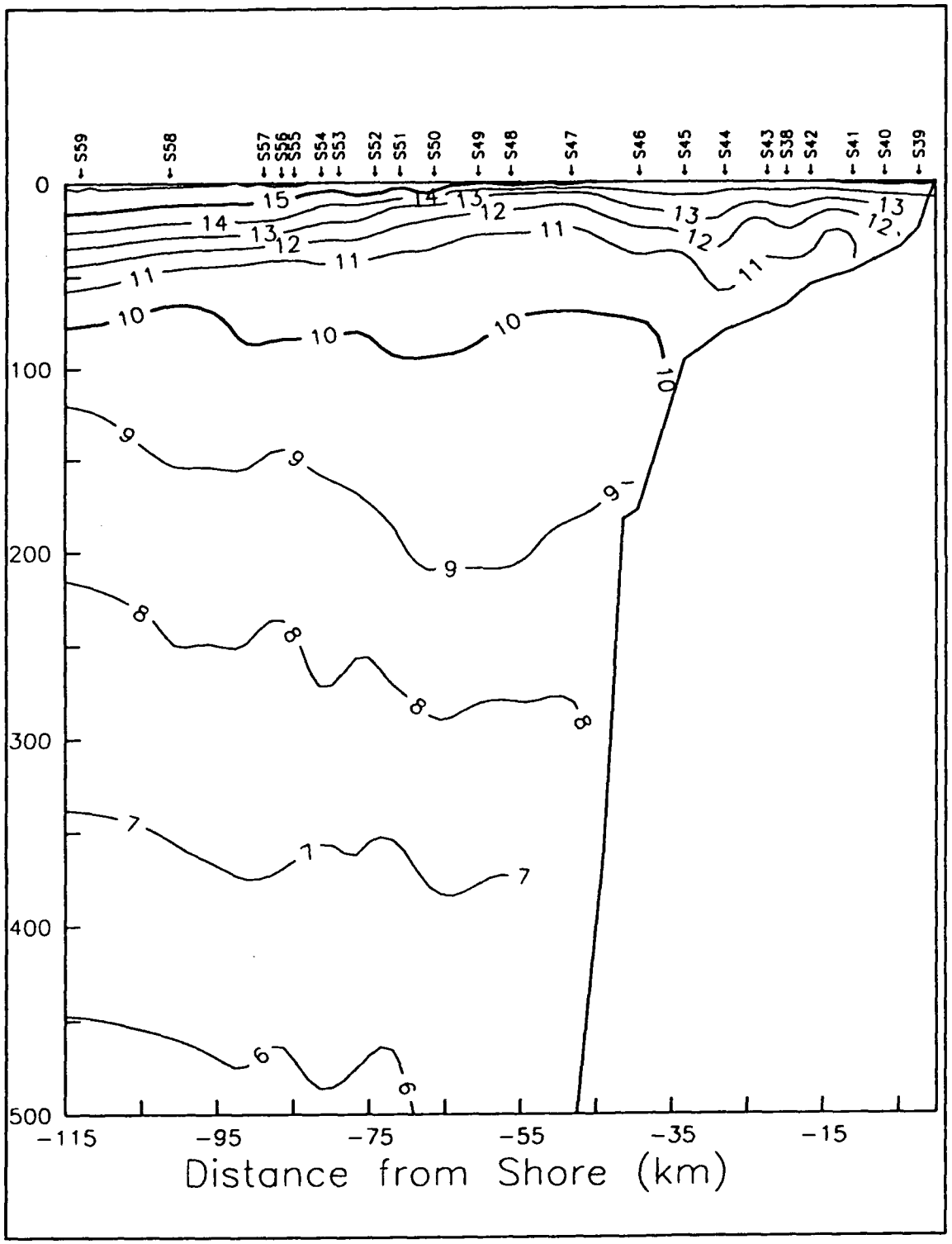

Figure 6a. Pioneer Transection Temperature Field: Temperatures in °C along the Pioneer Transection. CTD station locations are indicated along the top of the figure.

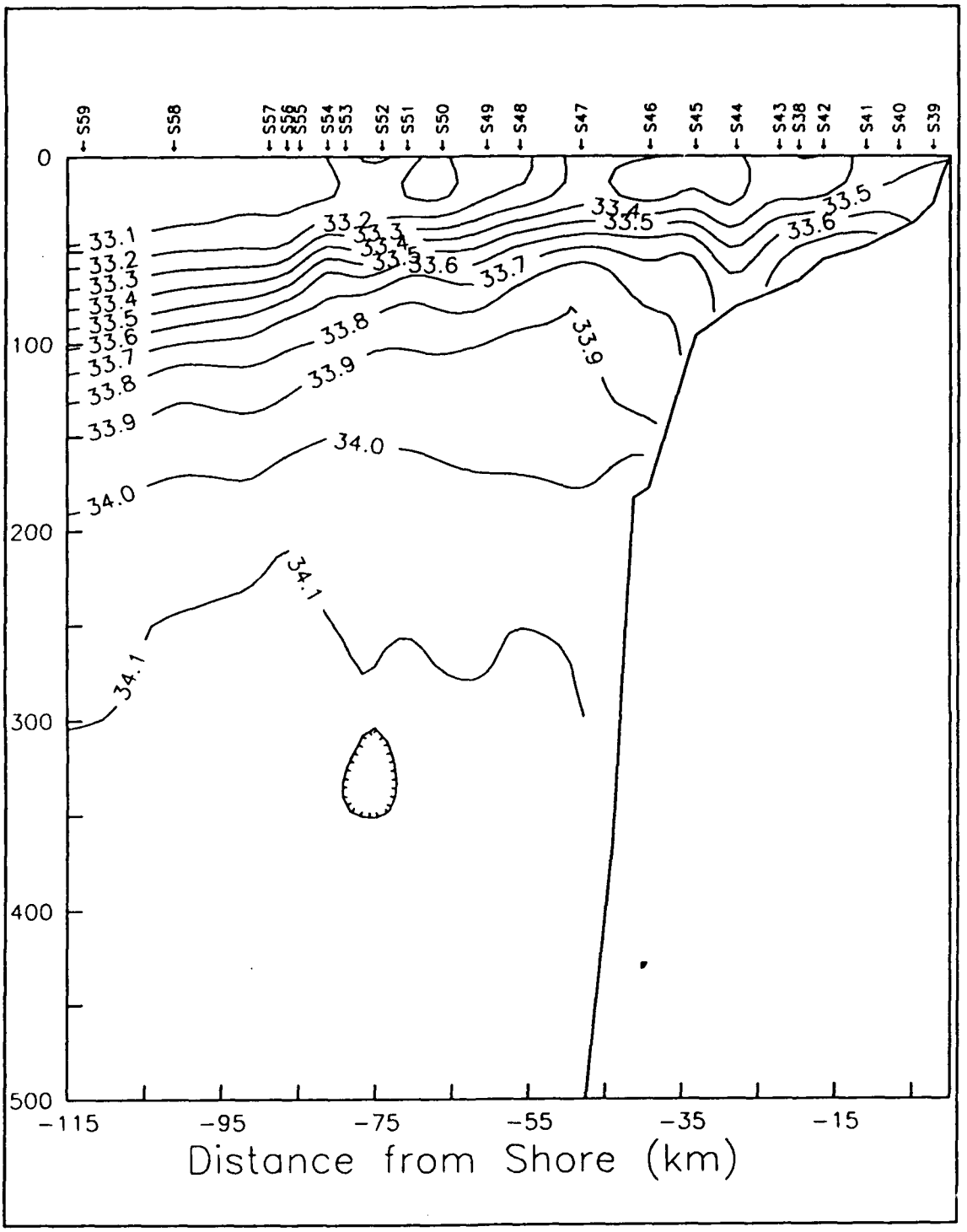

Figure 6b. Pioneer Transection Salinity Field: Salinities in psu along the Pioneer Transection. CTD station locations are indicated along the top of the figure. Hatching indicates a minimum.

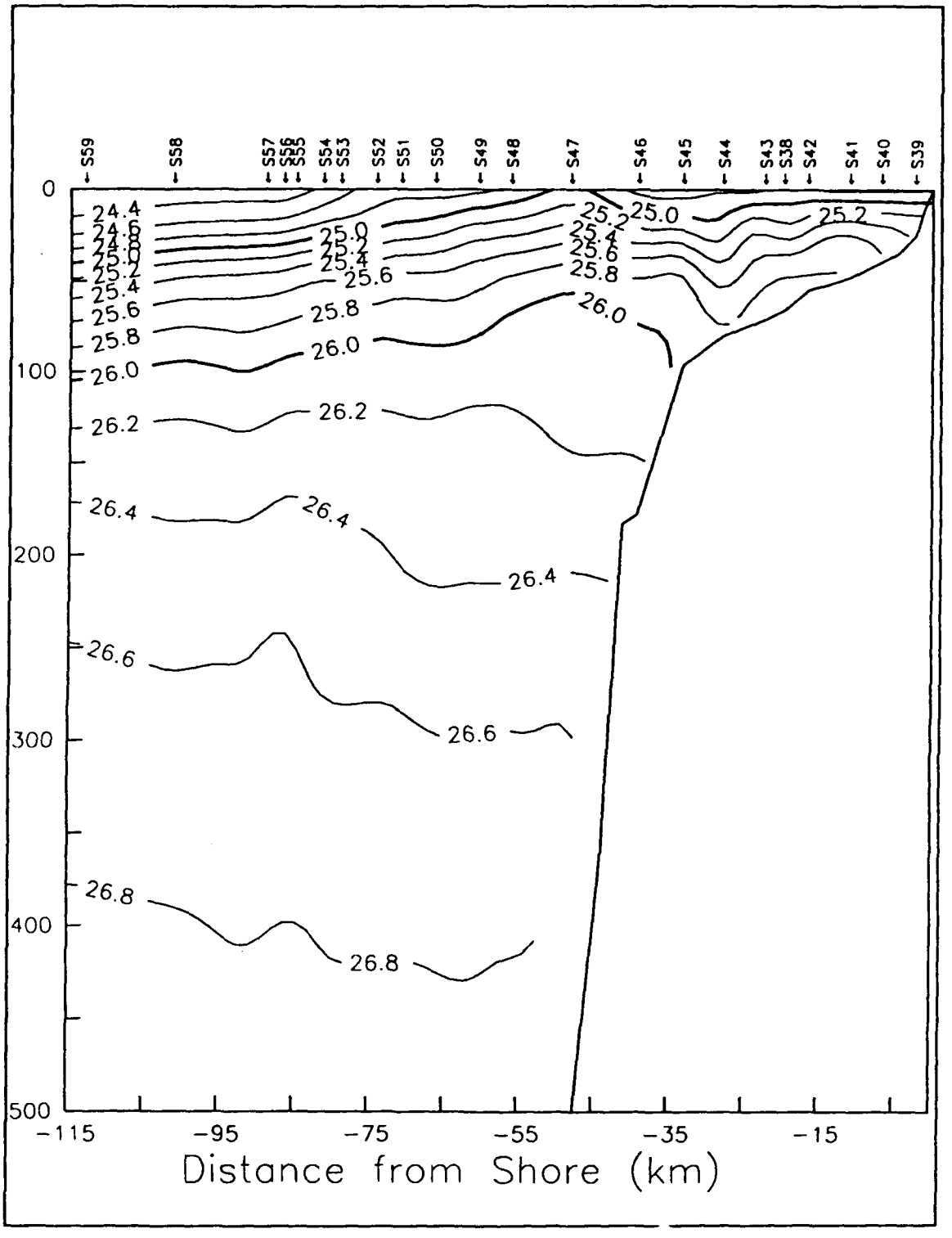

Figure 6c. Pioneer Transection Density Anomaly Field: Density anomaly values in kg/m^3 along the Pioneer Transection. CTD station locations are indicated along the top of the figure.

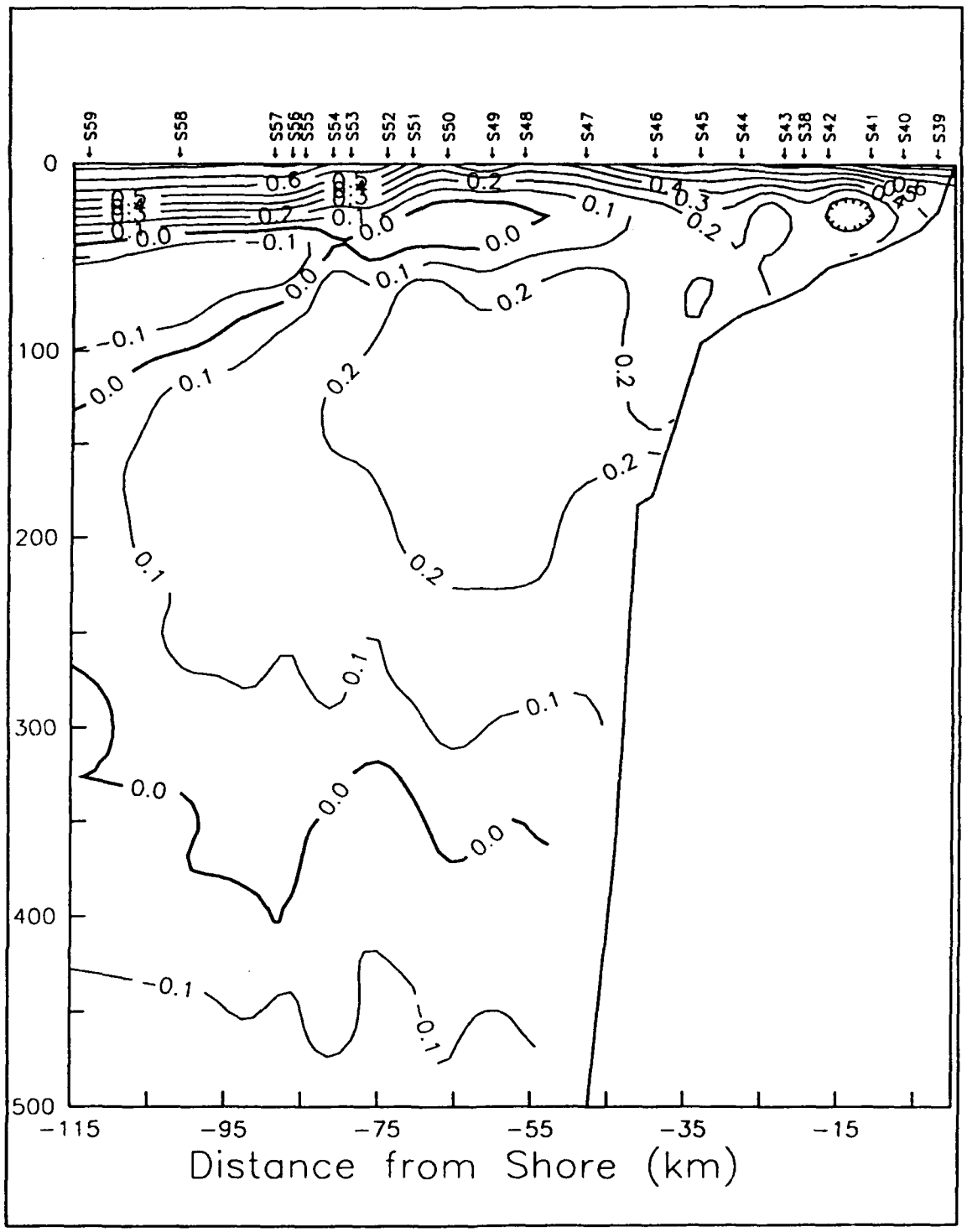

Figure 6d. Pioneer Transection Spiciness Field: Spiciness values along the Pioneer Transection. CTD station locations are indicated along the top of the figure. Hatching indicates a minimum.

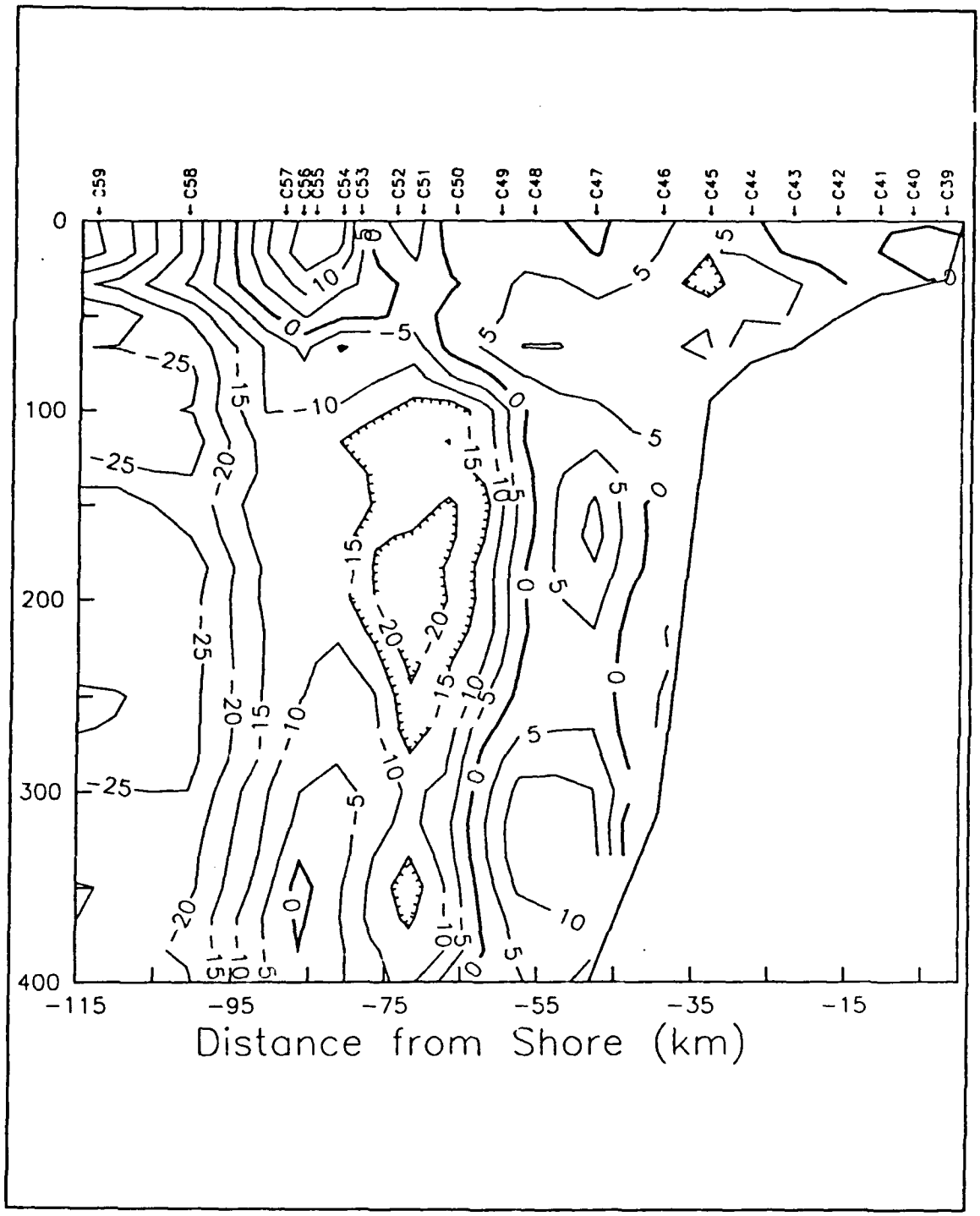

Figure 6e. Pioneer Transection Detided ADCP East-West Velocity: East-west velocity in cm/s along the Pioneer Transection. Positive values indicate eastward velocities. CTD station locations are indicated along the top of the figure. Hatching indicates a minimum.

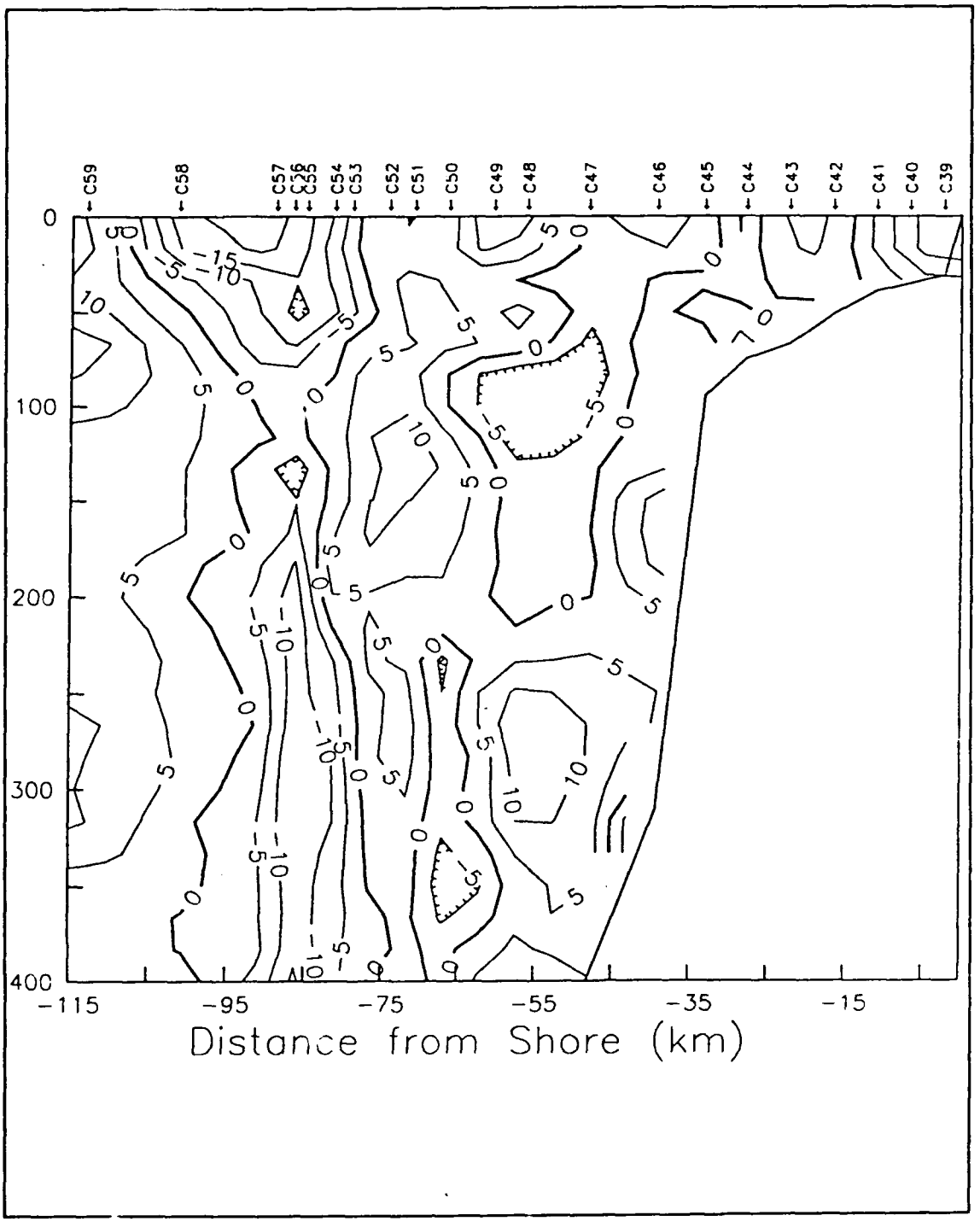

Figure 6f. Pioneer Transection Detided ADCP North-South Velocity: North-south velocities in cm/s along the Pioneer Transection. Positive values indicate northward velocities. CTD station locations are indicated along the top of the figure. Hatching indicates a minimum.

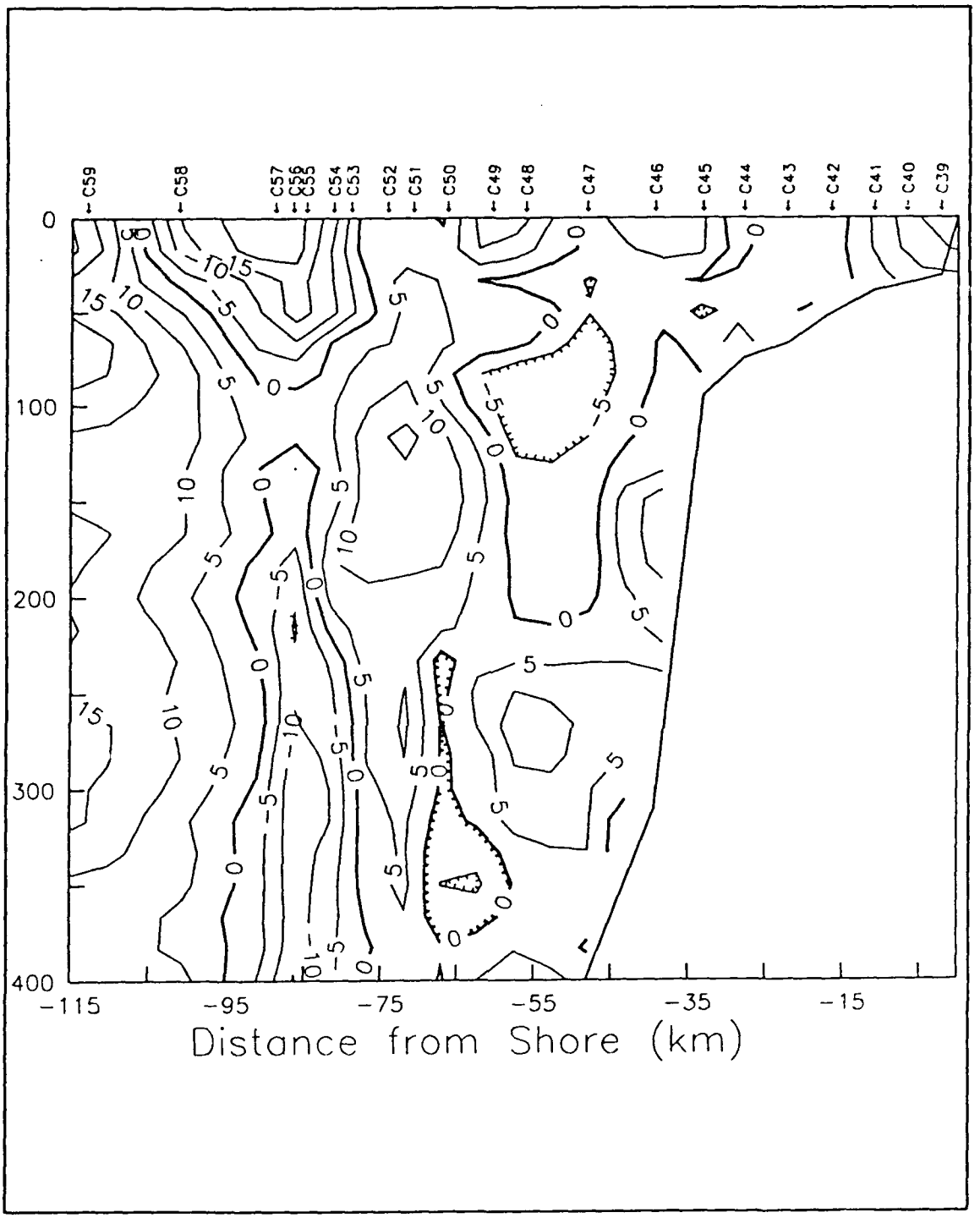

Figure 6g. Pioneer Transection Detided ADCP Cross Velocity: Cross - transection velocities in cm/s along the Pioneer Transection. Positive values indicate north-northwestward flow. CTD station locations are indicated along the top of the figure. Hatching indicates a minimum.

from 210m at station 59 to 285m at station 47. As with the Farallones transect, this is indicative of warmer waters of equatorial origin. This pattern is much less pronounced below 400m, where the 6.5C isotherm appears nearly level.

2. Salinity

Surface salinities fall generally into two regimes, greater than 33.3 and less than 33.2, the former occurring inshore of station 47 and the latter occurring offshore of station 48. In the upper 150m, the isohalines slope upward from station 59 to the coast; for example, the 33.5 isohaline is found at 92m at station 59 and at a depth of 4m at station 39. This steady rise from offshore toward the coast is interrupted between stations 47 and 44 over the upper slope and outer shelf where the isohalines slope downward toward the coast. Over the mid-shelf, a lens of bottom water of 33.7 psu is found.

In the region between about 50 and 200m, isohalines slope upward toward the coast (opposite to isotherms), indicating saltier water inshore. This pattern changes deeper in the water column. Between 300 and 500m, salinities are nearly constant.

3. Density

The pattern of isopycnals is similar to that of isotherms. Above about 100m, isopycnals upwell toward the coast and below 100m, they slope downward toward the coast.

For the shallower isopycnals, the exception is the region over the upper slope and outer continental shelf where isopycnals slope down toward the coast as well. This pattern reflects poleward flow at depth and over the upper slope and outer shelf (Robson, 1990).

4. Spiciness

The spiciness field is dominated subsurface by a region of large positive values, greater than 0.2, which is centered at a depth of about 150m adjacent to the continental slope. Above this maximum, a minimum occurs at the base of the seasonal thermocline; this minimum decreases toward shore. This spiciness minimum is located beneath the salinity minimum.

5. Detided East-West ADCP velocity

A region of divergence is marked by the zero isotach at about station 49. To the west of station 49, velocities are westward, with maximum speeds of 30 cm/s at station 59. Over the slope and outer shelf, velocities are eastward, with a peak velocities of 10 cm/s at the shelf break (station 45). The east-west component of flow is weak over the inner shelf.

6. Detided North-South ADCP velocity

The north-south velocity field is generally weaker and marked by alternating bands of northward and southward flow which are 10-20km wide. The strongest flows are next to the coast at stations 39 and 40 where northward flow greater than

15 cm/s is observed, and at depth over the slope (stations 46 and 47) and above 100m at station 59 where flow exceeds 10 cm/s. The strongest southward flow was observed at and just to the west of Pioneer seamount where flow at the surface exceeded 20 cm/s.

7. Detided Cross-Section ADCP velocity

Flow out of the section (southeastward) occurred over Pioneer seamount and above 100m over the upper slope and outer shelf. Elsewhere, flow is into the section (northwestward).

E. SATELLITE IMAGE OF GULF OF FARALLONES

The satellite image shown in Figure 7 was taken from the NOAA-11 satellite AVHRR Sensor at 1509 PDT on 15 August 1990.

Nearshore fog is evidenced by the lack of contrast at the coast. However, immediately offshore there is a band of cold water extending about 20 km offshore, as denoted by the darkest shading.

Sea surface temperature is warmer offshore (lighter shading). One of the interesting features in the image is the intrusion of a warm plume of water (15-16°C) southwest of the Gulf, about 40 km offshore. This feature is probably a meander or extrusion from the California Current. The northeast portion of this feature extends toward the Golden Gate and has a surface temperature in the range 14-15°C. Even though the image was taken five days after the hydrographic survey, the

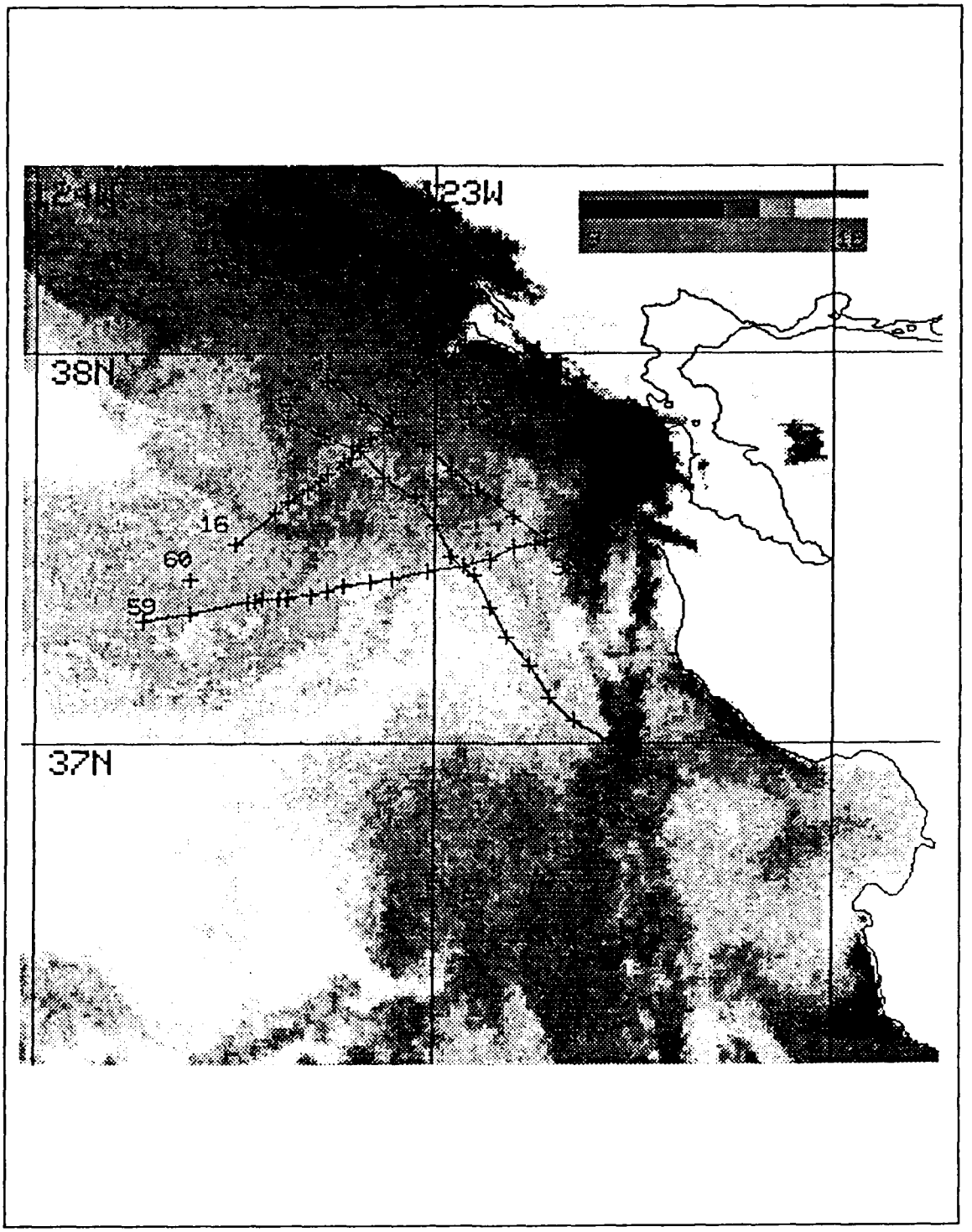

Figure 7. Sea Surface Temperature Pattern: Sea surface temperatures in °C for the Gulf of Farallones on August 15, 1990. This image is from the AVHRR sensor of the NOAA-11 satellite.

warm water was observed at the offshore stations both in the Farallones and Pioneer transections.

F. SUMMARY OF OBSERVED FLOW

The general pattern of flow in the Gulf of the Farallones was out of the Gulf at stations which lay along the northwestern perimeter and into the Gulf at southeastern stations. A strong region of shear was found just north of a shallow fresh water lens at station 10. In the Gulf, this shear zone was also a region of convergence; in 300m of water, it appeared to be a divergence. The fresh water lens appeared to be moving onshore.

Subsurface and offshore water appears to have the character of equatorial water associated with the California Undercurrent. For the Pioneer transection, the poleward flow appeared well organized. At the Farallones transection, the density field indicated a more complicated structure.

G. SALINITY MINIMUM

Both satellite imagery and velocity observations suggest that the low salinity lens observed at stations 10 and 36 is moving onshore. What is the source of this lens of fresh water; San Francisco Bay or surface waters farther offshore? To attempt to answer this question, I have plotted the temperature and salinity characteristics of the upper 50m of CTD casts where the difference between the surface salinity

and the subsurface minimum exceeded 0.2 psu (Figure 8). This included stations 48 through 52 as well as stations 10 and 36. Note that station 48 lies offshore of station 36, and falls upon a line which joins stations 48, 36 and 10 (Figure 2). The other four stations lay immediately offshore station 48 along the Pioneer transection. The fact that these stations lay adjacent to one another implies continuity in the origin and propagation of the salinity minimum.

Figure 8 shows that, except for station 52, which has about the same minimum salinity as station 49, the minimum salinity decreases with distance from shore. The density anomaly also follows this pattern. Processes which control water properties in this area in summer are heating and upwelling. Heating might favor warmer waters offshore if coastal fog persisted during the day. Upwelling occurs close to shore, where saltier and cooler subsurface waters are brought to the surface. Below the upper ocean boundary layer (which is 4-6m thick in these examples), mixing tends to occur along isopycnal surfaces.

The combination of these processes favors shoreward advection of this feature. As the water column is advected onshore, waters mix with upwelled waters, and salinity increases.

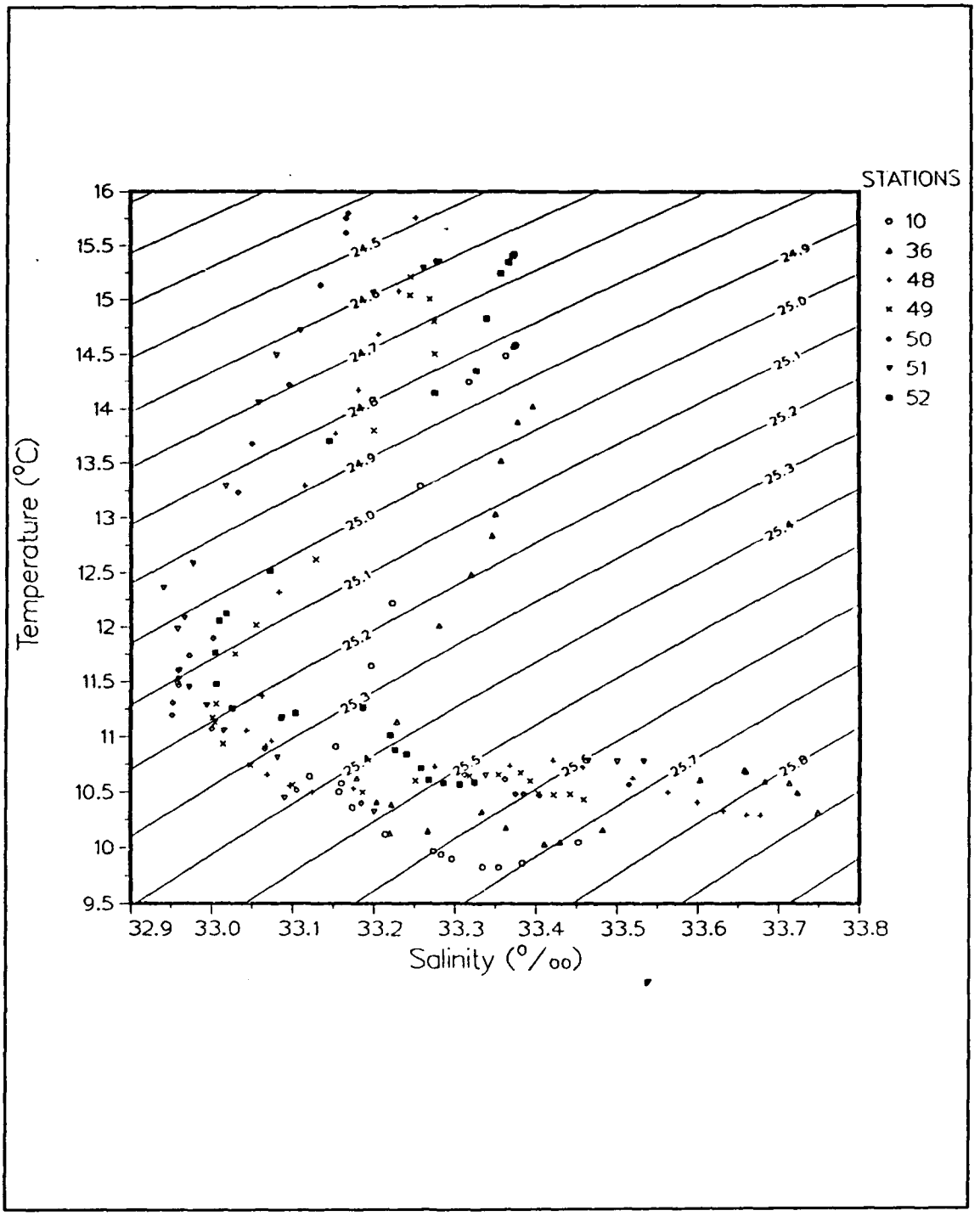

Figure 8. Temperature and Salinity Properties of Salinity Inversions: Only stations where the difference between sea surface salinity and the salinity minimum was 0.2 psu or greater are shown. Temperature and salinity values are shown for the upper 50m.

V. MIXING AND TRANSPORT FOR THE GULF OF FARALLONES

Having discussed the general hydrographic conditions in the region, I will next try to quantitatively estimate the role of the Gulf of Farallones in mixing fresh and salt water in the region. My motivation for these estimates is to try to better understand the mixing in the Gulf as well as the exchange with offshore waters.

A. VOLUME TRANSPORTS

If the enclosed volume between the coast and the Farallones, Inshore, and Pioneer transections is considered, then conservation of mass in this volume requires

$$V_i\rho_i + R + P = V_o\rho_o + E \qquad (5\text{-}1)$$

Here V_i is the transport into the volume, ρ_i the density of the water transported into the volume, V_o and ρ_o the corresponding quantities for flow out of the volume, R is fresh water flowing from San Francisco Bay into the Gulf, and P and E, respectively, the precipitation and evaporation from the surface area of this volume (Pickard and Emery, 1982). Since densities vary by less than 3%, they can be neglected, and volumes considered,

$$V_i + R + P = V_o + E \qquad (5\text{-}2)$$

The volume of fresh water entering San Francisco Bay can be estimated from daily records of the Department of Water

Resources (personal communication). The average daily flow for the period 5-10 August 1990 was 5342.2 ft^3/s or 149.8 m^3/s.

There was no precipitation in the region during our cruise. Evaporation has been estimated from both our shipboard meteorological observations and historical climatology. Evaporation is derived by dividing evaporative heat flux, Q_e, by the latent heat of evaporation, L_t,

$$E = \frac{Q_e}{L_t} \qquad \textbf{(5-3)}$$

A computer program developed by Roland W. Garwood, Jr. (personal communication) was used with meteorological observations at hydrographic stations. Required data included wind speed, air and sea surface temperatures, and dew point temperature. Figure 9 summarizes wind conditions during the cruise. This yielded an average evaporation of 8.951×10^{-6} kg/m^3-s or a total evaporation of 1.588×10^4kg/s or 15.5 m^3/s. Monthly tabulations of climatological data (Nelson and Husby, 1983) yield 19.8 m^3/s. The NOAA data buoy in the Gulf of Farallones could normally be used for yet another estimate of the evaporative flux but it was not operating during early August.

Volume transport can be estimated by integrating the detided ADCP velocity component, V_c, which is normal to the transections which bound the volume, from surface to bottom and from Pt. Reyes to Pt. San Pedro (see Figure 2 for the location of these sections),

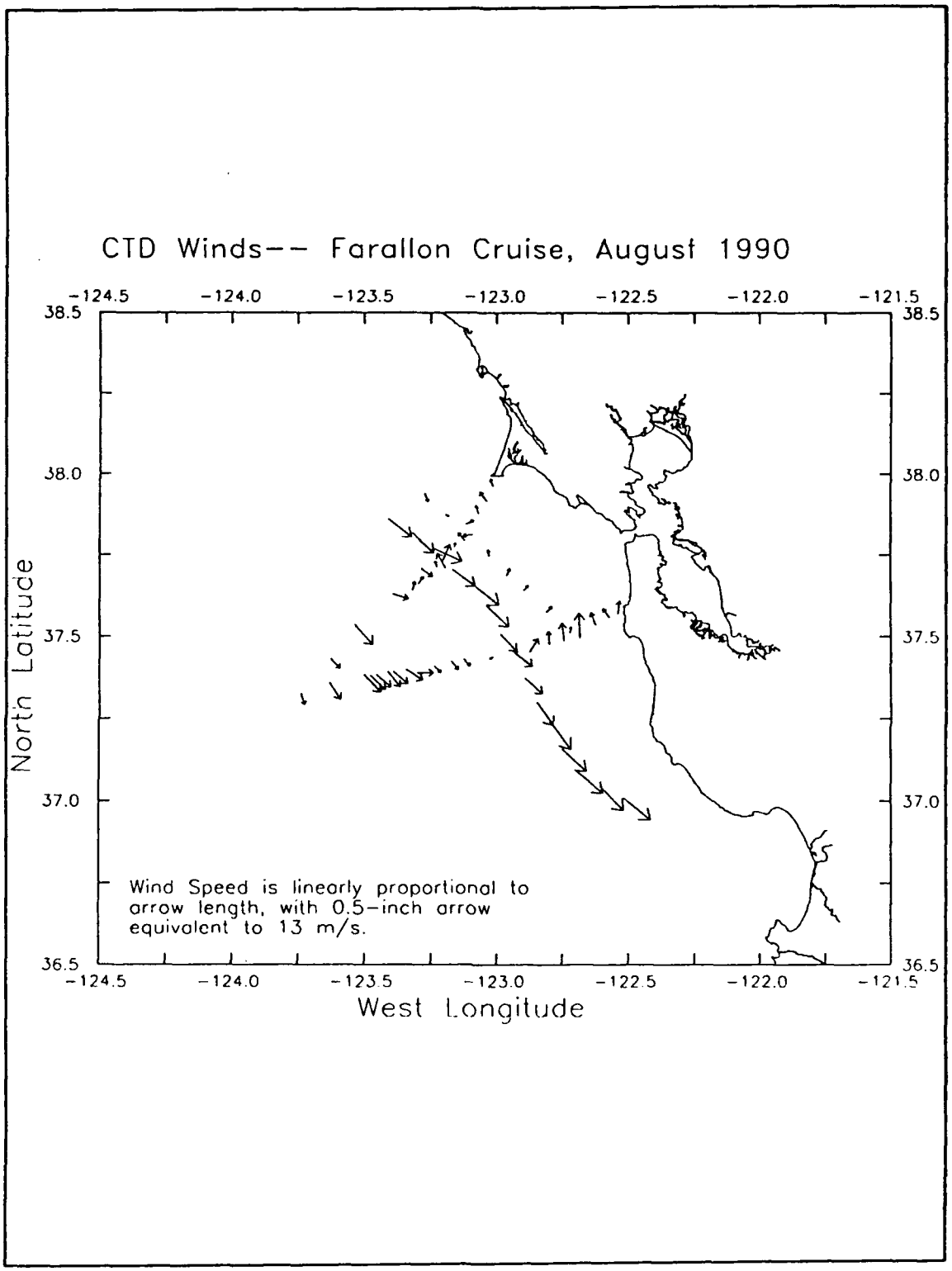

Figure 9. Winds observed at Hydrographic Stations: R/V Pt. Sur, 5-10 August 1990.

$$\int_{stn30}^{stn39} \int_{0}^{bottom} V_c dz dx = -138,212\ m^3/s, \qquad (5\text{-}4)$$

i.e. transport out of the volume is about 0.1 Sv (1 Sv = 10^6 m^3/s). As a check on this sum, we used the observed data (not detided) which yielded -243,555 m^3/s. A bias of 1 cm/s would yield a transport of 46,911 m^3/s.

Figure 10a shows the detided V_c used for this estimate. Negative velocities indicate that flow is out of the Gulf. The general trend is flow into the Gulf in the south and out of the Gulf to the north. The transition from flow out of the box to flow into the Gulf occurred between stations 35 and 36. Strongest flow out of the Gulf occurred at the surface at Pt. Reyes, about 48 cm/s. The strongest flow into the Gulf occurred at 40m at station 37, 28 cm/s. Flow in the upper 20m at station 34 was into the Gulf.

I also estimated the volume transport for the volume bounded by the Farallones, Offshore, and Pioneer transections. This yielded a transport of -726,014 m^3/s.

B. SALT BUDGETS

1. Total Volume

Salt budgets can be derived from the above equations by multiplying the transports into and out of the section by the corresponding salinities, S_i and S_o, so

$$V_i S_i + R + P = V_o S_o + E \qquad (5\text{-}5)$$

The salt flux can be estimated directly from detided cross section velocities and CTD salinities,

$$\int_{stn30}^{stn39} \int_{o}^{bottom} V_c S \, dz dx = -4{,}656{,}634 \ \ psu\text{-}m^3/s \qquad (5\text{-}6)$$

The difference between maximum and minimum salinties is 0.458 psu or about 1%; this means that the pattern of salt flux is the same as the velocity field. Salt is advected out of the Gulf to the north of station 35 and into the Gulf to the south of station 35. (The quantity $V_c S$ is not plotted).

If we assume that the lack of conservation of volume (mass) is due to an error, V_e, in the ADCP measurements over the area,

$$A = \int_{stn30}^{stn39} \int_{o}^{bottom} dz dx = 4.7 \times 10^6 \ m^2 \qquad (5\text{-}7)$$

Then substituting in (5-2) and adding an error term,

$$150 \ m^3/s = 138{,}212 \ m^{3/s} + 15.5 \ m^3/s + A \ V_e$$

and solving for V_e,

$$V_e = -138{,}078 \ m^3/s \ / \ 4.7 \times 10^6 \ m^2 = -3.0 \ cm/s$$

A corrected velocity, V'_c, is obtained

$$V'_c = V_c - V_e$$

Also note

$$V_e = \overline{V_c} = \frac{1}{A} \int_{stn30}^{stn39} \int_{o}^{bottom} V_c \, dz dx = -3.0 \ cm/s. \qquad (5\text{-}8)$$

Figure 10b shows V'_c. The effect of the correction has been to shift the zero isotach at station 35 northward about 3 km and

to decrease (increase) speeds to the north (south). The resulting salt flux,

$$\int_{stn30}^{stn39} \int_{o}^{bottom} V_c' S \, dzdx = -22{,}000 \; psu\text{-}m^3/s \qquad \textbf{(5-9)}$$

is about two orders of magnitude less than the salt flux derived from V_c but still negative. This indicates a net flux of fresh water into the Gulf.

Further decomposition of the salinity field into mean and perturbation terms yields a trival result. Consider

$$S = \overline{S} + S', \; where$$

$$\overline{S} = \frac{1}{A}\int_{stn30}^{stn39} \int_{o}^{bottom} S \, dzdx = 33.528 \; psu. \qquad \textbf{(5-10)}$$

Then,

$$\int_{stn30}^{stn39} \int_{o}^{bottom} V_c' S \, dzdx = \overline{S} \int_{stn30}^{stn39} \int_{o}^{bottom} V_c' \, dzdx + \int_{stn30}^{stn39} \int_{o}^{bottom} V_c' S' dzdx \qquad \textbf{(5-11)}$$

The middle term is zero, so the perturbation term balances (5-9), -22,000 psu-m^3/s.

Salt (S′) and salt flux ($V_c'S'$) are illustrated in Figures 10c and 10d, respectively. The isohalines for perturbation salinity are also similar to those for salinity, but vertical stratification results in negative values for the upper part of the water column and positive values at depth. The perturbation salt flux indicates flux out of the Gulf below 30m north of station 34 and above 30m between station 35 and 38. Salt flux into the Gulf occurs above 30m north of station 34 and below 30m between stations 35 and 38. Inshore of station 42, the flux is neglible.

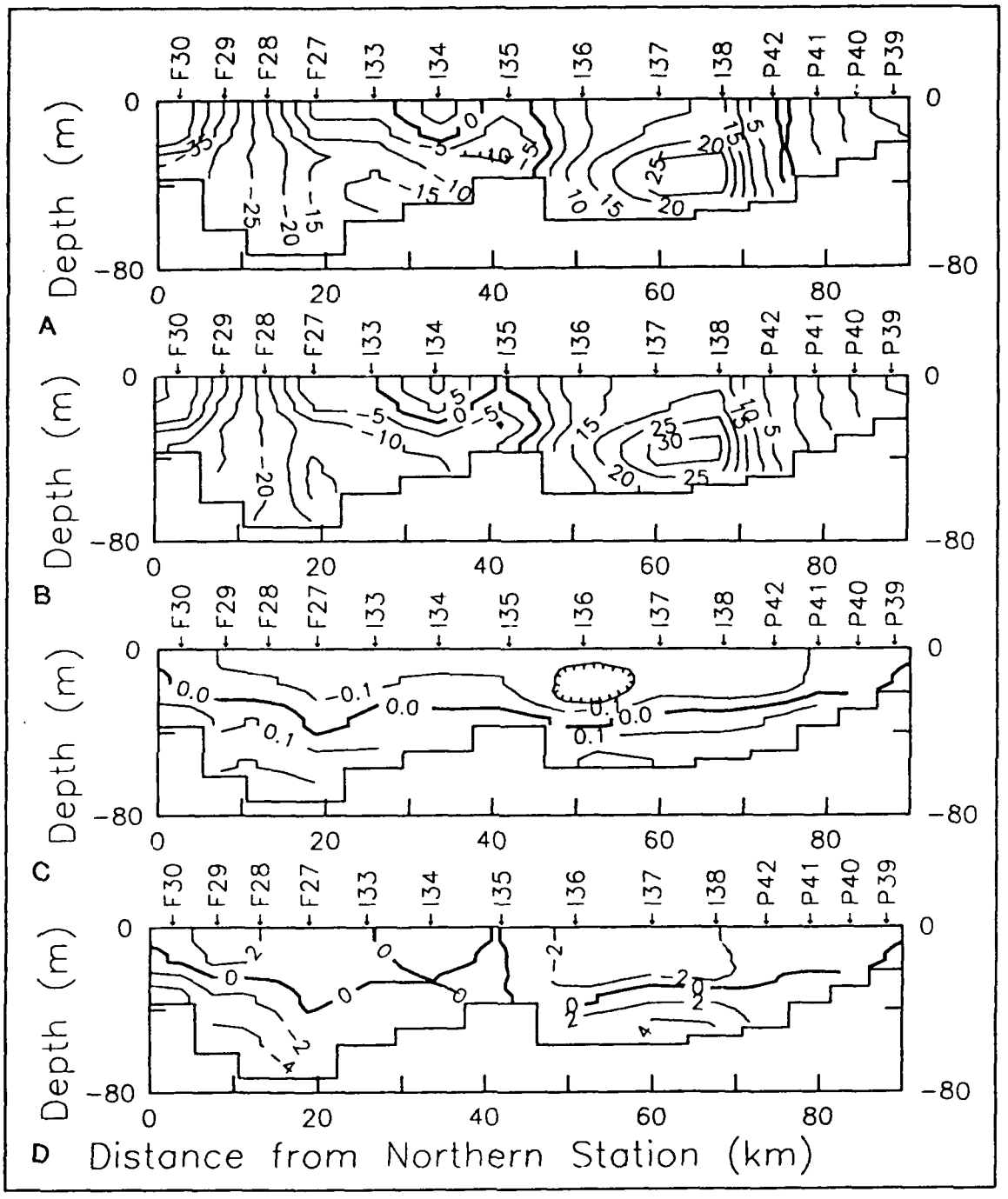

Figure 10. Salt Flux Quantities Around the Gulf of the Farallones: (a) Detided cross-transection velocities in cm/s. Positive values indicate flow into the Gulf. Hatching indicates a minimum. (b) Detided cross-transection velocity with mean removed in cm/s. (c) Salinity field with mean removed S' in psu. (d) Salt flux field V'_cS' in psu-cm/s. Positive values denote flux into the Gulf.

2. Layers

For this volume, I have also decomposed the salt flux into three layers. The surface layer extends from the surface to 19m, the middle layer from 20 to 39m, and the bottom layer from 40m to the ocean bottom. This modifies the salt conservation equations to include interfacial transport between layers,

$$\int_{coastline}^{inshore\ t.} \int_{pio.t.}^{far.t.} W_z S_z dxdy \sim \overline{W_z}\ \overline{S_z}\ A_z \qquad (5\text{-}12)$$

where W is vertical velocity, the subscript z indicates values at the depth of the interface z, and overbars indicate horizontal averages on the interface. Note that this assumes that $W'_z S'_z$ is negligible and that $\overline{S_z}$ can be estimated from the hydrographic sections. The modified salt balance equations are

Upper Layer:

$$P-E+R+A_{19}\,\overline{W_{19}}\,\overline{S_{19}} = \int_{stn30}^{stn39}\int_{0}^{19} V'_c S\ dzdx = 783774.3\ psu\text{-}m^3/s \qquad (5\text{-}13)$$

Middle Layer:

$$-A_{19}\,\overline{W_{19}}\,\overline{S_{19}} + A_{39}\,\overline{W_{39}}\,\overline{S_{39}} = \int_{stn30}^{stn39}\int_{19}^{39} V'_c S\ dzdx = -33680.8\ psu\text{-}m^3/s \qquad (5\text{-}14)$$

Bottom Layer:

$$-A_{39}\,\overline{W_{39}}\,\overline{S_{39}} = \int_{stn30}^{stn39}\int_{39}^{bottom} V'_c S\ dzdx = -772063\ psu\text{-}m^3/s \qquad (5\text{-}15)$$

The flux in the surface layer is out of the Gulf. The flux in the lower layers is into the Gulf. A_{19} and A_{39} are 1.58 x 10^9 m^2

and 1.12×10^9 m^2, respectively. To solve for $\overline{W_z}$, I have estimated $\overline{S_z}$ as

$$\overline{S_z} = \frac{1}{D} \int_{stn30}^{stn39} S_z \, dx \qquad \textbf{(5-16)}$$

where D is the distance from station 39 to station 30 along the transections.

Solving for the vertical velocity into the upper layer yields

$$W_{i9} = 1.5 \times 10^{-5} \text{ m/s}$$

and, for the vertical velocity from the lower into the middle layer,

$$W_{39} = 2 \times 10^{-5} \text{ m/s}$$

The equation for the bottom layer provides a check on the above estimate, yielding the same result! This is consistent with upwelling rates.

C. RESIDENCE TIME

The residence time, T, for waters from San Francisco Bay in the Gulf of the Farallones is simply the volume of the Gulf divided by the transport of these waters, i.e.

$$T = \frac{Volume}{Inflow} = \frac{7 \times 10^{10} \, m^3}{2.8 \times 10^5 \, m^3/s} = 2.5 \times 10^5 \sim 3 \; days$$

Here I estimated the volume of the Gulf as the sum of the volume of the three layers used above. Inflow is the sum of the positive flow across the sections. The result, three days,

indicates that waters in the Gulf are renewed on a synoptic time scale. Note that this assumes complete exchange and mixing and hence, provides the shortest possible residence time.

VI. CONCLUSIONS

Analysis of moored current meter data indicate that diurnal tides dominate the shelf in the Gulf of the Farallones but that semi-diurnal tides dominate on the slope. This result is consistent with previous studies (Noble, 1990). Using tidal constituents, I was able to detide ADCP data, improving the estimate of volume transport by a factor of two.

The circulation pattern observed in the Gulf of Farallones was a cyclonic system of flow. Water entered the Gulf from south of the Farallon Islands and exited the Gulf between Pt. Reyes and the Farallon Islands. This pattern is confirmed by a satellite image which indicates a tongue of warm water penetrating into the Gulf from offshore as well as the increasing salinity and density along a shallow salinity minimum in this area. This cyclonic flow was also observed by previous current meter moorings in and near the Gulf. Note that this circulation would provide a return flow to balance offshore flow which has been observed at Pt. Reyes.

Over the slope and below 200m, water mass characteristics and isopycnal slopes indicate the presence of the California Undercurrent. Along the Pioneer transection, the poleward flow occurs from the slope to Pioneer seamount. At the Farallones section, isopycnal slopes indicate this poleward

flow reverses, although ADCP data indicate persistent poleward flow in the region.

Volume transport calculations yielded 0.14 Sv of flow out of the Gulf. Since this value should be close to zero, an error of about 3 cm/sec is likely in the ADCP data. Estimates of salt flux for the region indicate a flux of about -22,000 psu-m^3/s. This indicates a small volume of freshwater flow onto the shelf. A lower bound on the residence time for the region was 3 days.

LIST OF REFERENCES

Chelton, D.B., "Seasonal Variability of Alongshore Geostrophic Velocity of Central California," *Journal of Geophysical Research*, v. 89, pp. 3473-3486, May 1984.

Chelton, D.B., Bernstein, A. Bratkovich, and P.M. Kosro, "Central California Coastal Circulation Study, Transections," *American Geophysical Union*, v. 68, pp. 1, 12-13, 1987.

Conomos, T.J., "Properties and Circulation of San Francisco Bay Waters," *San Francisco Bay, The Urbanized Estuary*, pp. 47-84, T.J. Conomos, ed., Pacific Division of AAAS, San Francisco, 1979.

Denbo, D.W., et al., "Current Meter Observations Over the Continental Shelf Off Oregon and California, Feb. 1981-Jan 1984," Reference 84-12, College of Oceanography, Oregon State University, November 1984.

Minerals Management Service, "Final Report, California Seabird Ecology Study: Satellite Data Analysis," V. II, 1987.

Flament, P., "A Note on Seawater Spiciness and Diffusive Stability," unpub. man., 1986.

Foreman, M.G.G., "Tidal Analysis Program Package," Pacific Marine Science Report 78-6, Institute of Ocean Sciences, 1978.

Hickey, B.M., "The California Current System - Hypotheses and Facts," *Prog. Oceanog.*, v. 8, pp. 191-279, 1979.

Kosro, P.M., "Shipboard Acoustic Doppler Current Profiling During the Coastal Ocean Dynamics Experiment," Ph.D. Dissertation, S10 Ref. 85-8, Scripps Institutions of Oceanography, 1985.

Moschovos, J.S., "Compare at Sea Position Using Mini-Ranger,, Loran C (Internav) in the Context of Measuring Current Velocity with Shipboard ADCP," Master's Thesis, Naval Postgraduate School, Monterey, California, December 1989.

Nelson, C.S., and D.M. Husby, "Climatology of Surface Heat Fluxes Over the California Current Region," NOAA Technical Report, NMFS SSRF-763, 1983.

Noble, M., "A Preliminary Report on Currents Over the Slope off San Francisco Bay," U.S. Geological Survey, unpublished, 1990.

Noble, M., and G. Gelfenbaum, "A Pilot Study of Currents and Suspended Sediment in the Gulf of Farallones," *U.S. Geological Survey,* in press, 1990.

Pickard, G.L., and W.J. Emery, *Descriptive Physical Oceanography,* Pergamon Press, Oxford, 1982.

Pollard, R. and J. Read, "A Method for Calibrating Shipmounted Acoustic Doppler Profilers and the Limitations of Gyro Compasses," *Journal of Atmospheric and Oceanic Technology,* v. 6-6, pp. 859-865, 1989.

Robson, A.J., "Circulation of the California Undercurrent Near Monterey in May 1989," Master's Thesis, Naval Postgraduate School, Monterey, California, June 1990.

Strub, et al., "Seasonal Cycles of Currents, Temperatures, Winds and Sea Level Over the Northwest Pacific Continental Shelf 35°N to 48°N," *Journal of Geophysical Research,* v. 92, pp. 1507-1526, 1987.

Unesco Technical Papers, *Marine Science,* v. 4, p. 101, United Nations Educational Scientific and Cultural Organization, 1987.

INITIAL DISTRIBUTION LIST

		No. Copies
1.	Defense Technical Information Center Cameron Station Alexandria, Virginia 22304-6145	2
2.	Library, Code 52 Naval Postgraduate School Monterey, California 93943-5002	2
3.	Dr. Curtis A. Collins, Code OC/Co Naval Postgraduate School Monterey, California 93943	2
4.	Dr. Marlene Noble U.S. Geological Survey Mail Stop 79 345 Middlefield Road Menlo Park, California 93025	1
5.	LT.j.g. Erhan Gezgin İnönü Cad. No. 209/26 35360 Izmir/TURKEY	1
6.	Dz. K.K. Deniz Harp Okulu Kütüphanesi Tuzla - ISTANBUL/TURKEY	1
7.	Dz. K.K. Seyir Hidrografi ve Oşinografi Dairesi Beykoz - ISTANBUL/TURKEY	1
8.	Dr. Toby Garfield, Code OC/Gf Naval Postgraduate School Monterey, California 93943	1
9.	Dr. Ed Uber Farallones National Marine Sanctuary Fort Mason San Francisco, California	1
10.	Prof. Leslie Rosenfeld, Code OC/Ro Naval Postgraduate School Monterey, California 93943	1

11. Dr. Frank Schwing 1
Pacific Fisheries Environmental Group
P.O. Box 831
Monterey, California 93942

12. Dr. William van Peeters, Code 2032WP 1
Naval Facilities Engineering Command
Western Division
P.O. Box 727
San Bruno, California 94066